The Dissertation Committee for Haley Joy Finley-Jones Certifies that this is the approved version of the following dissertation:

Improving Figures of Merit and Expanding Applications for Inductively Coupled Plasma Mass Spectrometry

Committee:

James A. Holcombe, Supervisor

Richard M. Crooks

Katherine A. Willets

Chris M. Sparks

Karen S. Browning

.Jennifer S. Brodbelt

Improving Figures of Merit and Expanding Applications for Inductively Coupled Plasma Mass Spectrometry

by

Haley Joy Finley-Jones, BS

Dissertation

Presented to the Faculty of the Graduate School of

The University of Texas at Austin

in Partial Fulfillment

of the Requirements

for the Degree of

Doctor of Philosophy

The University of Texas at Austin

August, 2010

Dedication

For my parents, who taught me that I should never allow my education to diminish my ability or desire to learn.

Acknowledgements

First and foremost, I would like to acknowledge my advisor, Professor James A. Holcombe. His extensive knowledge-base and excellent public speaking skills have truly been an inspiration. Because of him, I have gained a full appreciation of "seeing the forest through the trees" and counting statistics. I would like to acknowledge former lab members, John Molloy, Adam Rowland and Carina Gunder for their support and guidance. Thank you also to current members Isaac Arnquist and Shelly Casciato. It has been a pleasure, and I will always remember our lunchtime discussions fondly. As you finish graduate school, keep these words in mind: "If we knew what it was we were doing, it would not be called research." – Albert Einstein

I would like to acknowledge my family for supporting me through 20 years of school. And last but not least, I would like to thank my husband for his ability to make me laugh in just about any situation.

Improving Figures of Merit and Expanding Applications for Inductively Coupled Plasma Mass Spectrometry

Publication No._____

Haley Joy Finley-Jones, Ph.D.

The University of Texas at Austin, 2010

Supervisor: James A. Holcombe

Although inductively coupled plasma mass spectrometry (ICP-MS) is generally considered a reliable analytical technique, increasing demands on its capabilities require continued research and improvements. ICP-MS is susceptible to both matrix effects and drift, leading to a decline in accuracy and precision. A number of techniques are routinely used to compensate for these issues. Internal standardization is one such solution that requires relatively simple sample preparation and yet offers the possibility of improving both accuracy and precision. In order to be effective, an optimal analyte/internal standard pair must be chosen. Traditionally, analyte/internal standard pairs are chosen based on similarities in mass and/or ionization potential. The present studies sought to develop a program that determined standards based on the minimization of analytical error. 102 masses were monitored over 27 perturbations, *i.e.*, changes to sample matrix and operating parameters. The standard deviations of the analyte/internal standard ratios were then used as a measure of internal standard performance. A thorough statistical analysis was conducted to determine trends between a good

analyte/internal standard pair and similarities in chemical property. Similarities in mass offered the strongest relationship to a good internal standard choice, although many exceptions existed. The program was then tested over time and multiple instrument optimizations as well as on a completely different ICP-MS instrument. Results of these tests suggest that the data originally collected for the prediction program is not instrument-specific and thus provided a broader base of useful applications.

Due to its unmatched sensitivity and multielement capabilities, ICP-MS is frequently utilized for biological samples. A more recent application, however, seeks to use ICPMS for the purpose of determining specific associations between metals and proteins. Such speciation requires a high resolution and reproducible separation prior to ICPMS analysis. Gel electrophoresis offers good separation and is well matched with the scanning properties of laser ablation sample introduction. The present study utilized native gel electrophoresis coupled with a uniquely modified electroblot system to improve sensitivity and to elucidate additional information. Chemically modified quartz fiber filters were successfully used as the transfer membrane to improve protein and metal capture efficiency.

Table of Contents

List of Tables

List of Figures

Chapter 1: Introduction

1.1 Inductively Coupled Plasma Mass Spectrometry

Inductively coupled plasma mass spectrometry (ICP-MS) was introduced commercially in 1983[1, 2] and is widely accepted as the most powerful trace metals analysis tools available. It is capable of 5-7 orders of magnitude linear dynamic range, ppq detection limits and allows multielement detection with virtually complete coverage of the periodic table. Initially, the sample is introduced into an Ar plasma where it is atomized and ionized at 7,000-10,000 K. The ions are extracted from the plasma through sample and skimmer cones and then move through system via ion optics. Once they reach the mass spectrometer they are separated by m/z and ultimately detected. Although typically considered a mature technique, analysis by ICP-MS is complicated by several limitations. As with any mass spectrometric method, isobaric interferences are problematic. Besides the isobars between elements and their isotopes, ICP-MS suffers from the presence of isobars from polyatomic ions. These are typically ions containing 2 or 3 atoms and frequently involve the major constituents in the plasma, e.g., Ar, N, O, etc. Additionally, samples with an elevated matrix component can also produce polyatomics, generally with major plasmas gas components, e.g., ArC^+, $NaAr^+$, NaO^+, etc. High resolution sector field mass spectrometers can overcome some of these interferences at the cost of multielement capabilities. Collision or reaction cells are another means of reducing Ar^+ and various polyatomic isobaric interferences, but the collision cells also generally reduce the detection efficiency for the analyte ions.

1.1.1 Sample Introduction

Surprisingly, the transfer of sample to the plasma is not a trivial matter and is often considered the Achilles heel of ICP-MS analysis. While techniques have been developed for solution, slurry and solid samples, solutions are the most common sample form. Sample aspiration into a nebulizer to form a fine aerosol is used for sample introduction. There are a variety of nebulizer designs available, including those that are capable of slurry analysis. Most nebulizers, however, have a low tolerance for sample particulates and are easily clogged. Once the sample aerosol is created, a spray chamber eliminates all but the smallest droplets. Although this helps to improve S/N by minimizing the solvent load, it also greatly reduces sampling efficiency. The most common pneumatic nebulizer, for example, exhibits a sampling efficiency of only 1-2% [3] for sample aspiration rates of 1-2 mL/min. This requires sample sizes on the order of milliliters, which is limiting for samples such as biological fluids that may not be available in milliliter quantities. With reduced liquid flow rates, delivery efficiencies to the plasma can increase significantly. However, many of these high efficiency nebulizers are very prone to clogging and provide minimal, if any, sensitivity improvement.

Laser ablation is utilized for solid samples with virtually no sample preparation requirements. It works by focusing a pulsed laser beam onto the sample, which leads to large power densities that are capable of vaporizing even refractory materials. He or Ar gas are used to transport the vaporized sample to the plasma torch. Because it requires little to no sample preparation, there is less risk for contamination. Laser ablation also allows for spatial resolution that is not possible with other ICP sample introduction techniques. It therefore has applications in mapping the metal content of a given sample.

The major limitation of laser ablation ICP-MS lies in quantitation. There are few samples with matrix matched standards available, so laser ablation introduction is largely limited to qualitative, semiquantitative and isotope ratio applications.

Electrothermal vaporization operates similar to the electrothermal atomization that is used for atomic absorption. A furnace, generally made of carbon or metal filament, is electrically heated to desolvate and vaporize the sample before it is carried by Ar gas to the plasma. Unlike electrothermal atomization, it is not necessary to completely atomize molecules within the sample. Electrothermal vaporization is capable of introducing liquid, slurry and solid samples. Sampling efficiency is significantly higher than that of a nebuilzer and therefore sample volumes on the order of microliters are all that are required. By removing much of the matrix before introduction, the load on the plasma can be greatly reduced along with a number of the argon-matrix ion interferences. Despite these benefits, ETV-ICP-MS has never gained comparable popularity to the other sample introduction methods discussed.

1.1.2 Ion Formation

The Ar plasma acts as a high temperature ionization source for the mass spectrometer. It is formed and held at the end of a quartz torch consisting of three concentric tubes and situated within an induction coil. Once the Ar gas is flowing, free electrons produced by a spark igniter intiatiate the avalanche breakdown by colliding with and ionizing Ar atoms as they are accelerated within the RF field of the induction coil. Tangential flow of Ar gas in the outermost concentric tube of the torch provides gas that thermally contains the plasma and prevents the torch from melting. Sample is

introduced through the narrow central channel of the torch to the base of the plasma. As the sample moves through the different temperature zones of the plasma, it is desolvated, atomized and ultimately ionized. The plasma effectively ionizes most of the elements on the periodic table with an efficiency of >90%.[4] Atoms with a high first ionization potential (e.g. As and Be) exhibit lower ionization efficiency while other elements with low first and second ionization potentials (e.g. Ba) will have a small number of ions in the +2 charge state.

Both ions and neutral gas are subsequently extracted via pressure differential through the ~1 mm opening of a sampling cone and continue through the small orifice of a skimmer cone. This skimmer is followed by a negatively charged ion lens or third skimmer, which removes negatively charged ions as well as electrons, thus creating a positive ion beam that is steered by the ion optics to the mass analyzer.

1.1.3 Mass Analyzer and Detection

There are several types of mass analyzers that can be coupled to an ICP ion source. The most common mass analyzer design for commercially available instruments is the quadrupole. A typical ICP quadrupole is made of four parallel rods. An RF potential is applied between each pair of rods while a superimposed DC potential creates an oscillating electric field. As ions traverse down the center of these rods, only those at a specific m/z ratio will exhibit a stable trajectory, ultimately reaching the detector, while the others will be lost by impaction with the rods. As the applied RF and DC potentials are scanned, different ions with different m/z ratios will be detected. Thus, any given potential nominally results in only one m/z reaching the detector. The ratio of the time

spent monitoring a given m/z relative to the scan time is referred to as its duty cycle. Although quadrupole mass analyzers offer excellent sensitivity when monitoring a relatively small number of masses, analytical performance can drop rapidly as the number of analytes increases. The duty cycle limitations are exacerbated when a transient technique is being monitored such as that produced by electrothermal vaporization, chromatographic separations or when laser ablation is used either for spatial mapping or in a single pulse mode of operation. The most common detector used with a quadrupole mass analyzer is an electron multiplier or channeltron.

Double focusing, or high resolution mass analyzers are utilized primarily in applications that require the highest accuracy in isotope ratios or to eliminate elemental isobaric and polyatomic interferences. Initially, ions are accelerated through a curved electrostatic field that focuses the ions while unifying their kinetic energies. The focused beam of ions then traverses across a magnetic field that deflects the ions with a curvature specific to each m/z ratio. The number of masses that can be monitored is limited by the type of detection system used. A series of Faraday cups offer good sensitivity and the most accurate isotope ratio measurements. However, they also limit the multielement capabilities to only a handful of similar masses.

Time-of-flight (TOF) mass analyzers are the least common among commercially available ICP-MS instruments. Ions are accelerated via push-out plate into a field-free flight tube in discrete packets. If the kinetic energy is same for all ions in a packet, their migration velocity is dependent only their m/z ratio. However, a given ion's proximity to the push-out plate at the time of release causes a spread in kinetic energies that is detrimental to resolution. A reflectron (or ion mirror) is used to compensate for this

spread in kinetic energy, thus vastly improving resolution. TOF mass analyzers provide complete m/z coverage at every push-out event, making them well suited for multi-element detection and transient events. Although quadrupoles offer more sensitivity for a small number of masses monitored, the TOF excels when larger m/z coverage is required. A discrete dynode electron multiplier is the most common ion detector.

1.2 IMPROVING ANALYTICAL ACCURACY AND PRECISION

Analytical accuracy is defined as the level of similarity between a measured value and the *true* value. Errors in accuracy can originate at virtually every stage of analysis; from sample preparation to mass-dependent variations in the efficiency of an electron multiplier [5]. The plasma itself is prone to matrix effects that can significantly alter output signals. These changes in analyte signal may be subsequently misinterpreted as changes in concentration. A large number of studies have looked into the effects that result from both high and low ionization potential matrix elements.

Analytical precision is the spread of measured values and can be numerically represented as a standard deviation. Poor precision in ICP-MS results is typically attributed to plasma flicker and drift but can also arise during sample introduction. Several techniques have been developed to improve the accuracy and precision of ICP-MS analysis.

1.2.1 Standard Addition

Standard additions are commonly used to correct for matrix effects. A sample is split into multiple aliquots and the analyte(s) are added via standard in increasing

concentration to all but one sample aliquot. All samples are run and the analyte output signal is plotted vs. the known concentration of added standard. Extrapolation of the x-intercept offers the unknown analyte concentration in the sample free of standard. The literal combination of sample and calibration curve provides perfect matrix matching and ultimately leads to more accurate concentration measurements. Although very effective in correcting accuracy, it does nothing to improve precision and is commonly combined with other methods that do so. Sample preparation is relatively time consuming, and large sample size requirements may be limiting for certain applications (e.g., biological fluids).

1.2.2 Isotope Dilution

Isotope dilution is highly effective for improving both accuracy and precision. Sample preparation is simple but can have the large sample amount requirements of standard. An isotopically enriched analyte standard is added to the sample at a known concentration; referred to in this context as a spike. Using the resulting ICP-MS signal, atomic masses and known isotope abundances, the concentration of unknown analyte can be determined. Unfortunately, this technique is not applicable for monoisotopic species such as ^{75}As and ^{59}Co. It can also be cost prohibitive since enriched isotopes are needed for each analyte of interest.

1.2.3 Internal Standardization

An “ideal internal standard” shares chemical and physical properties with the analyte of interest that result in proportional signal responses between the two species.

Under this condition, internal standardization is capable of providing improvements in both accuracy and precision. Isotope dilution is an example of near ideal internal standardization since the internal standard and analyte are isotopes of the same element. Despite its potential, internal standardization is primarily used to improve precision with hopes that some compensation of matrix interferences might also be minimized. It is not unusual to utilize internal standardization in combination with standard addition or matrix matching in an attempt to correct for both matrix interferences and drift. When doing so, researchers often use a single internal standard such as ^{115}In[6-8] or ^{103}Rh[9,10] for all analytes.

For internal standardization, sample preparation is relatively simple and inexpensive. A known and consistent amount of internal standard is added to all samples and external calibration standards. Once the data is collected, the analyte/internal standard ratios of the calibration standards are plotted on the y-axis as opposed to output signal, and concentration is plotted on the x-axis. The major challenge of this technique lies in choosing an ideal or optimal internal standard. There are two requirements that must be met in making this choice: 1) The internal standard cannot be present at varying concentrations within the samples; and 2) the analyte/internal standard ratio should remain constant for any given concentration ratio despite changes to the matrix or instrument fluctuations. If both of these conditions are met, then changes to the analyte/internal standard ratio are solely reflective of a change in analyte concentration. Several studies have cited the importance of internal standard choice for ICP-MS [11-14]. It is common among the ICP-MS community to make the selection based on similarity in mass and/or ionization potential.[11, 12] The research presented in Chapter 2 and 3 utilizes a statistical approach based on the minimization of analytical error in order to predict

optimal analyte/internal standard pairs under a variety of operating conditions that are used to simulate real-world samples.

1.3 CHARACTERIZATION OF METALLOPROTEIN COMPLEXES

The balance of essential metals within an organism plays an important role in many biological functions. To emphasize this importance, it is estimated that one in three proteins are complexed with a metal ion. In contrast to the static nature of the genome, the cellular metallome is highly dynamic and dependent on its environment. Metal association is largely a matter of "degree," measured quantitatively by the K_f of the metal-protein complex. In addition to the protein-metal complexes of interest, it is expected that many metals will complex with functionalities on the outside of the protein, probably contributing little to protein activity. Furthermore, it is likely that the protein composition and metal content of a cell is dependent on the specific growth stage of a cell's life. The dynamic nature of this system creates a challenging problem for researchers attempting to elucidate and characterize protein-metal interactions. The importance of this characterization, however, has been frequently noted in the literature.[15-19]

As is often necessary in analytical development, it is important to differentiate between the ideal and the currently possible. An ideal tool would allow researchers to determine metal protein interactions *in vivo*, so as not to disrupt the cellular equilibrium of free vs. complexed metal ions. To date, the technique for determining protein-metal interactions requires that the cell be lysed and the proteins separated prior to analysis. Thus, the protein-metal equilibria may be vastly altered, particularly in the instance of

labile metalloproteins. Since the form (e.g., oxidation state, extent of complexation, etc.) of the metals *within* the cell is impossible to determine, the *in situ* equilibrium between metal and protein cannot be predicted. Therefore, metallome characterization is currently limited to those complexes with large enough formation constants or with sufficiently slow dissociation kinetics to withstand the abrupt environmental change brought upon by cell lysing and protein separation. The most common means to date of characterizing these protein-metal relationships involves the isolation and analysis of a single protein.

1.3.1 Polyacrylamide Gel Electrophoresis

The excellent sensitivity and large linear dynamic range afforded by ICP-MS makes it ideally matched for the metals analysis of metalloproteins. However, the destructive nature of the plasma requires a reproducible, high resolution separation prior to introduction for the purpose of elucidating individual protein-metal associations. Column-like separations including capillary electrophoresis (CE) and high performance liquid chromatography (HPLC) have been successfully coupled to an ICP-MS for a wide variety of applications. A major limitation to both CE and nano-HPLC is that they are susceptible to sample overload.[20] Furthermore, CE is known to experience a substantial performance decrease resulting from the high salt matrices typical of protein buffers.[21] HPLC offers a relatively simple interface for ICPMS, but it is not capable of separating very large protein mixtures, such as those found within a cell. An alternative to column separation is polyacrylamide gel electrophoresis (PAGE). Once the protein solution is loaded into the wells at the top of the gel, a potential is applied. The proteins then migrate down the gel and are separated by mass and charge. In order to achieve this

separation, all the proteins must migrate in the same direction. A common solution is to use a charge shift molecule that binds to the protein and imparts a negative charge. Two commonly employed charge shift molecules are sodium dodecyl sulfate (SDS) and Coomassie Brilliant Blue, both of which will be discussed in more detail in subsequent sections.

In addition to 1-dimensional mass separation, multi-dimensional PAGE can be used to greatly enhance resolution. The most effective 2D PAGE separation utilizes isoelectric focusing (IEF) prior to the mass separation. Proteins are placed on a pH gradient strip and a potential is applied. The electric field causes the proteins to migrate until they reach a pH where they are electrically neutral. Thus, IEF separates proteins based on their isoelectric point. 2D-PAGE with SDS as the charge shift molecule is the only separation technique capable of separating hundreds of proteins in practice [22] The focus of this dissertation, however, will be limited to the 1D mass separation.

1.3.1.1 Denaturing PAGE

SDS is an ionic detergent that binds with high affinity to many different proteins and is effective at relatively low concentrations.[23-26] Its molecular structure is illustrated in Figure 1.1.

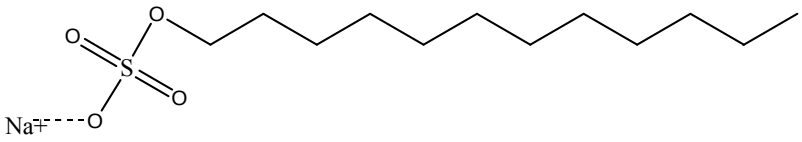

Figure 1.1: Molecular structure of SDS.

SDS can bind through its sulfate group to positively charged amino acid side chains and also through its alkyl chain to hydrophobic side chains, ultimately resulting 1.4 g SDS/g protein.[23] Unfortunately, it has been well established in recent literature that SDS cannot be used for labile complexes due to its denaturing characteristics.[27-29]

1.3.1.2 Native PAGE

There are two distinct methods of native gel electrophoresis; blue native (BN) and clear native (CN) PAGE. In 1991 Schägger and von Jagow introduced the technique of BN PAGE.[30] Coomassie Brilliant Blue™, traditionally used as a protein stain, was introduced as the charge shift molecule in lieu of SDS. Its molecular structure is illustrated in Figure 1.2.

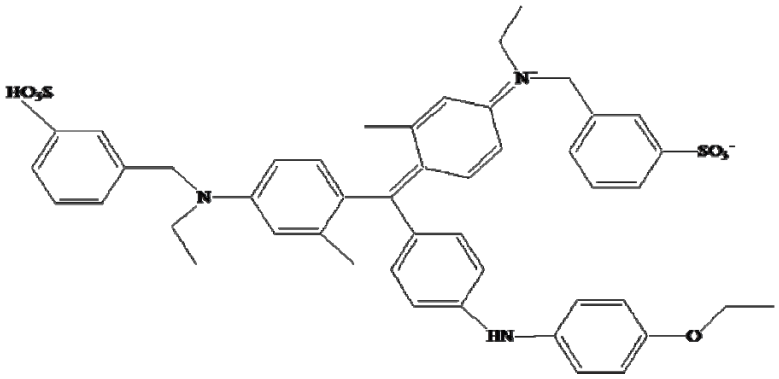

Figure 1.2: Molecular structure of Coomassie Brilliant Blue™.

Coomassie imparts a negative charge to the proteins without the strong denaturing effects of SDS. Unlike SDS, Coomassie binds specifically to the basic (Arg, His, Lys) and hydrophobic (Phe, Tyr, Trp) amino acids.[31] Therefore, the binding efficiency, and in turn, the charge shift efficiency of Coomassie to a given protein is dependent on the

number of exposed binding sites. Since BN PAGE does not efficiently dissociate subunits or aggregates and is at least partially dependent on protein shape, the resolution suffers as compared to SDS PAGE. Although BN PAGE has been utilized successfully in a number of metallomics studies,[29, 32-34] it is still unclear to what extent its presence may affect protein-metal binding.

CN PAGE offers the least invasive separation, utilizing no charge shift molecule. In a comparison study between BN and CN PAGE Wittig et al. found that enzymatic activity was better preserved when CN PAGE was used.[35] This comes at an obvious cost to resolution. In CN PAGE, the migration distance depends on shape, mass *and* charge at a near neutral pH, making calibration exceedingly difficult.

1.3.2 Equilibrium Considerations

Protecting the integrity of the metal-protein relationships before metal detection is crucial to metallomics research. Although metal loss from SDS[27-29] and staining[34] have been reported, there are other avenues for metal loss within this system. Since binding strengths vary greatly between metals and proteins, it is important to consider the impact of equilibrium during the separation. If a protein's local environment (e.g., running buffer) is metal-free and the "off rate" (e.g., dissociation rate constant) is fast then weakly bound metals will most likely dissociate from the proteins, and the correct metal-protein assignments will not be made. Loading the running buffers with metal shifts the equilibrium toward complexation and prevents metal loss. However, metal-loading the buffers may result in higher background signals in addition to possible incorrect assignments resulting from weak adsorption of metals from the solution to the

functionalities of the amino acids positioned, for example, on the outside of the proteins of interest.

1.3.3 Electroblotting

The use of an electroblot following BN PAGE offers a number of benefits to metallomics research. Electroblotting was initially developed to improve access to proteins for applications requiring molecular probes.[36] A diagram of a traditional electroblot system is depicted in Figure 1.3. The gel and transfer membrane are placed within an electric field, causing the negatively charged proteins to move through the gel in the z-direction and onto the membrane surface.

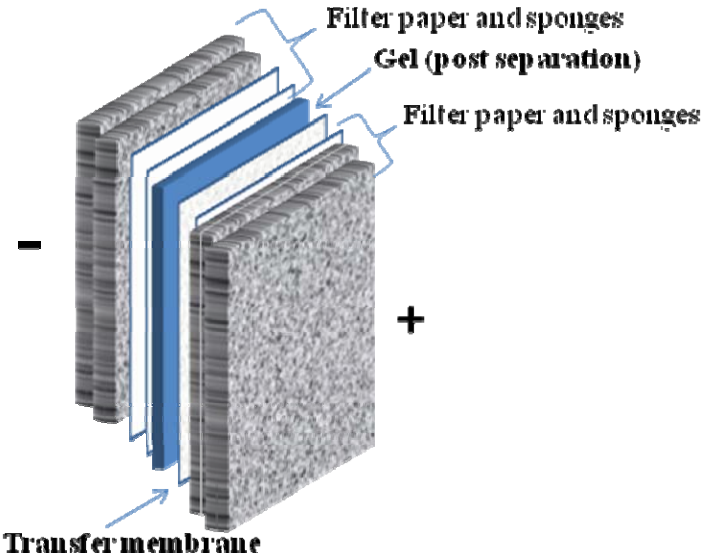

Figure 1.3: Diagram of a traditional electroblot.

The positively charged, free metal ions will move in the opposite direction, toward the cathode, thus significantly reducing background metal signal both from the gel and the

blotting membrane on the anode side of the gel. Adding a transfer membrane to the cathodic side would allow the capture of both proteins (anodic side) *and* free metals (cathodic side). Time-resolved studies utilizing capture at both the anode and cathode may offer insight into the binding strength and/or release kinetics between protein and metal. In order to ultimately gain this type of information, it is important to maximize the capture efficiency of the transfer membranes. The two most common transfer membranes are polylvinylidene fluoride (PVDF) and nitrocellulose. Evaluations of both PVDF[37] and nitrocellulose[38] have been reported in metallomics literature. Chemical modification of transfer surfaces may assist in maximizing capture efficiency, and thereby sensitivity. PVDF offers superior protein capture efficiency over nitrocellulose.[36] However, it does not offer particularly strong metal binding capabilities. Since PVDF is chemically inert, altering the chemical nature of the surface to improve capture efficiency is not trivial, although it has been done.[39] Glass fiber filters have also been evaluated as electroblot transfer membranes.[40, 41] However, taking advantage of the relative ease of modifying this SiO_2 surface has not been pursued. The current research (chapter 4) will explore this modification and evaluate its performance.

1.3.3.1 Chemical Modification of Electroblot Membranes

Data will be shown for three surface modifications of a Whatman quartz fiber filter. Acid hydrolysis, depicted in Figure 1.4, yields surface siloxyl groups, which can bind to free metals.

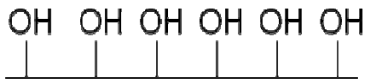

Figure 1.4: SiO_2 surface after acid hydrolysis.

Silanization with (3-mercaptopropyl)trimethoxysilane (3-MPS) yields surface thiol groups (Figure 1.5), which are known to bind strongly to the soft acid metals as well as a number of transition metals.[42] The exposed thiols of 3-MPS have also been used to capture large biomolecules.[43]

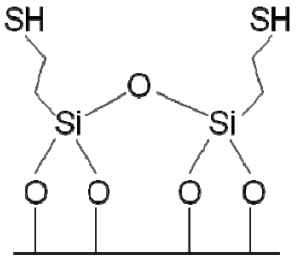

Figure 1.5: SiO_2 surface modified with 3-MPS.

Poly acrylic acid (PAA) was reported by Miller et al. as having relatively strong affinity for Cu^{2+},[44] which is found on a number of different proteins. Metal binding to PAA is through the terminal carboxylate groups (Figure 1.6). Initial steps in this immobilization require acid hydrolysis and silanization with 3-MPS. Since no attempt was made to cap any non-reacted thiols from 3-MPS, the mixed surface (thiol and PAA) may offer more comprehensive capture capabilities.

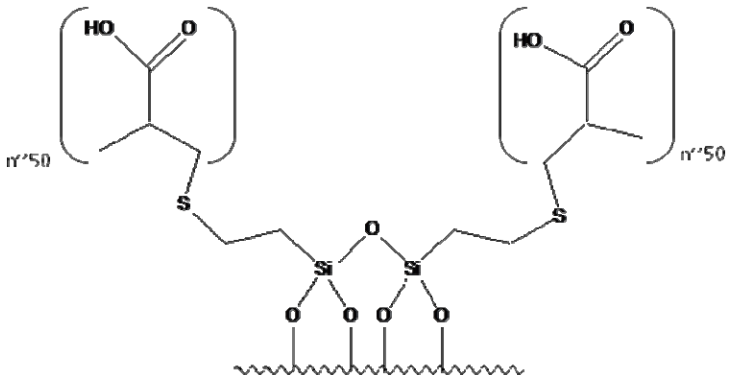

Figure 1.6: SiO_2 surface modified with PAA.

1.4 OVERVIEW OF DISSERTATION

Despite its superior capabilities and presence as a mature technique, increasing demands require that researchers continue to improve ICP-MS performance. The present work seeks to improve ICP-MS figures of merit and expand its utility in biological applications. Chapter 2 focuses on improving accuracy and prediction through the use of a novel internal standard prediction program. Chapter 3 determines the real-world utility of this program by testing it over time, instrument optimizations and across instrument platforms. Chapter 4 explores the use of laser ablation ICP-MS for the characterization of protein-metal interactions, highlighting the intricacies of such analysis. Chapter 5 offers a summary as well as a discussion of future directions.

1.4.1 Choosing Internal Standards for ICP-MS

Internal standards are routinely used with inductively coupled plasma mass spectrometry (ICPMS) to minimize the impact of signal instability. Previous studies

indicate that internal standard choice should be directed by similarities in mass, but they neglect to address the possibilities of exceptions or what impact a poor internal standard choice may have on quantitative results. A 51 element suite was run under varying instrument and matrix perturbations on an ICPMS instrument equipped with a time-of-flight mass spectrometer. Each element was ratioed to every other element for perturbed conditions that were intended to simulate variations in matrix composition or drift in operating parameters. These included changing sample delivery rate, matrices (NaCl and acetic acid) and horizontal torch position. The %RSDs of each analyte-to-internal standard ratio were used to rank the relative quality of each analyte-internal standard pair and their response to changing conditions. Multiple ordinary least squares equations were calculated to evaluate various chemical and physical properties that may be predictors of an optimal analyte-internal standard combination. Overall, similarity of masses was found to be the most important predictor of a good internal standard. However, exceptions did exist under various perturbations and among different elements. In a final study, nine analytes were run under perturbed experimental conditions and in two complex matrices (NaCl and acetic acid), but quantitation was attempted using simple aqueous standards. Accuracy and precision were evaluated for several internal standards for each of the nine elements as well for the nine analytes where no internal standard was employed. From this evaluation, it was clear that internal standard choice can have substantial effects on analytical accuracy and the improvement of analytical precision, but there is no single physical or chemical parameter that reliably allows *a priori* selection of a "good" internal standard for any given analyte.

1.4.2 Evaluation of Internal Standard Predictions

In a previous paper from this laboratory, 51 different elements were ratioed to each other under a variety of altered matrix and instrumental conditions. The objective was to isolate element pairs that made good internal standards for each other. The data were collected and evaluated using a nebulizer and an inductively coupled plasma time-of-flight mass spectrometer. Although results suggested that many optimal internal standards were correctly predicted, it was not clear whether these predicted internal standard pairs would remain good choices for this instrument over an extended time period and whether changing instrumental platforms would alter the internal standard selections. This paper considers the choice of previously selected "good" internal standards for several elements using the same GBC ICP(TOF)MS after several optimizations, a torch change and nebulizer replacement. It also considers the use of the previously determined "good" internal standards with an Agilent ICP(quadrupole)MS with a different nebulizer system, torch, mass analyzer, etc. Interestingly, it was found that the internal standards predicted in the initial study continued to perform well on both platforms considered in the present study. In fact, overall errors were smaller in the second set of TOF data and on the quadrupole than those in the first set of TOF data. Mass and ionization potential trends were also similar to those from the previous study. Although there remains to be an equation allowing *a priori* selection of the ideal internal standard, the current results suggest that the prediction program developed in the previous study is effective over time and instrumental platforms.

1.4.3 Determination of Labile Protein-Metal Relationships

The importance of determining and characterizing the interactions between proteins and metal ions is well established. There are a number of diseases (e.g., Alzheimer's disease and amyotrophic lateral sclerosis) with known associations to metalloproteins. The present study seeks to utilize a systematic approach toward developing an analytical technique with a focus on maintaining the equilibrium between free and bound metal ions. In order to test the reliability of this tool, analysis was limited to the well-characterized protein, bovine serum albumin. Blue native poly acrylamide gel electrophoresis followed by a modified electroblotting technique was utilized for the purpose of protein separation and metal preconcentration for improved S/N. Laser ablation inductively coupled plasma mass spectrometry was employed for trace metals analysis of the separated and electroblotted protein bands. Several surfaces were compared for protein and metal capture efficiency as well as ablation characteristics. Ablation directly from a dried gel resulted in low sensitivity compared with the ablation of an electroblot membrane. Chemically modified electroblot membranes were found to offer enhanced protein capture efficiency during the electroblot process.

1.5 REFERENCES

1. A. R. Date and A. L. Gray, *Analyst (Cambridge, United Kingdom)*, 1983, **108**, 159-165.

2. D. Douglas, *Canadian Research*, 1983, **16**, 55-56, 59-60.

3. R. F. Browner, *Chemical Analysis (New York, NY, United States)*, 1987, **90**, 244-288.

4. R. S. Houk, *Analytical Chemistry*, 1986, **58**, 97A-98A, 100A-105A.

5. A. Rowland and J. A. Holcombe, *Spectrochimica Acta, Part B: Atomic Spectroscopy*, 2009, **64B**, 35-41.

6. C. Vandecasteele, M. Nagels, H. Vanhoe and R. Dams, *Analytica Chimica Acta*, 1988, **211**, 91-98.

7. J. Wang, W. L. Shen, B. S. Sheppard, E. H. Evans, J. A. Caruso and F. L. Fricke, *Journal of Analytical Atomic Spectrometry*, 1990, **5**, 445-449.

8. J. Wang, E. H. Evans and J. A. Caruso, *Journal of Analytical Atomic Spectrometry*, 1991, **6**, 605-608.

9. M. Y. Perez-Jordan, J. Soldevila, A. Salvador, A. Pastor and M. de la Guardia, *Journal of Analytical Atomic Spectrometry*, 1999, **14**, 33-39.

10. M. Wang, *Yejin Fenxi*, 2004, **24**, 19-22.

11. J. J. Thompson and R. S. Houk, *Applied Spectroscopy*, 1987, **41**, 801-806.

12. F. Vanhaecke, H. Vanhoe, R. Dams and C. Vandecasteele, *Talanta*, 1992, **39**, 737-742.

13. X. Chen and R. S. Houk, *Journal of Analytical Atomic Spectrometry*, 1995, **10**, 837-841.

14. C. Sartoros and E. D. Salin, *Spectrochimica Acta, Part B: Atomic Spectroscopy*, 1999, **54B**, 1557-1571.

15. J. Szpunar, *Anal. Bioanal. Chem.*, 2004, **378**, 54-56.

16. R. Lobinski, D. Schaumloffel and J. Szpunar, *Mass Spectrom. Rev.*, 2006, **25**, 255-289.

17. W. Shi and M. R. Chance, *Cell. Mol. Life Sci.*, 2008, **65**, 3040-3048.

18. E. L. Que, D. W. Domaille and C. J. Chang, *Chem. Rev. (Washington, DC, U. S.)*, 2008, **108**, 4328.

19. S. Mounicou, J. Szpunar and R. Lobinski, *Chem. Soc. Rev.*, 2009, **38**, 1119-1138.

20. A. Prange and D. Proefrock, *Analytical and Bioanalytical Chemistry*, 2005, **383**, 372-389.

21. R. Lobinski, C. Moulin and R. Ortega, *Biochimie*, 2006, **88**, 1591-1604.

22. H. Chassaigne, C. C. Chery, G. Bordin, F. Vanhaecke and A. R. Rodriguez, *Journal of Analytical Atomic Spectrometry*, 2004, **19**, 85-95.

23. J. A. Reynolds and C. Tanford, *Proceedings of the National Academy of Sciences of the United States of America*, 1970, **66**, 1002-1003.

24. K. S. Rao and V. Prakash, *J. Biol. Chem.*, 1993, **268**, 14769-14775.

25. D. E. Otzen, *Biophysical Journal*, 2002, **83**, 2219-2230.

26. K. J. Tiefenbach, H. Durchschlag and R. Jaenicke, *Progress in Colloid & Polymer Science*, 2004, **127**, 136-147.

27. C. C. Chery, L. Moens, R. Cornelis and F. Vanhaecke, *Pure Appl. Chem.*, 2006, **78**, 91-103.

28. M. Garijo Anorbe, J. Messerschmidt, I. Feldmann and N. Jakubowski, *Journal of Analytical Atomic Spectrometry*, 2007, **22**, 917-924.

29. M. S. Jimenez, L. Rodriguez, M. T. Gomez and J. R. Castillo, *Talanta*, 2010, **81**, 241-247.

30. H. Schagger and G. von Jagow, *Anal Biochem*, 1991, **199**, 223-231.

31. T. Marshall and K. M. Williams, *Anal. Biochem.*, 1992, **204**, 107-109.

32. J. S. Becker, S. Mounicou, M. V. Zoriy, J. S. Becker and R. Lobinski, *Talanta*, 2008, **76**, 1183-1188.

33. J. S. Becker, D. Pozebon, V. L. Dressler, R. Lobinski and J. S. Becker, *Journal of Analytical Atomic Spectrometry*, 2008, **23**, 1076-1082.

34. A. Raab, B. Pioselli, C. Munro, J. Thomas-Oates and J. Feldmann, *Electrophoresis*, 2009, **30**, 303-314.

35. I. Wittig and H. Schagger, *Proteomics*, 2008, **8**, 3974-3990.

36. B. T. Kurien and R. H. Scofield, *J. Immunol. Methods*, 2003, **274**, 1-15.

37. M. Wind, I. Feldmann, N. Jakubowski and W. D. Lehmann, *Electrophoresis*, 2003, **24**, 1276-1280.

38. A. Polatajko, M. Azzolini, I. Feldmann, T. Stuezel and N. Jakubowski, *Journal of Analytical Atomic Spectrometry*, 2007, **22**, 878-887.

39. M. C. Clochard, N. Betz, M. Goncalves, C. Bittencourt, J. J. Pireaux, K. Gionnet, G. Deleris and A. Le Moel, *Nucl. Instrum. Methods Phys. Res., Sect. B*, 2005, **236**, 208-215.

40. R. H. Aebersold, D. B. Teplow, L. E. Hood and S. B. H. Kent, *J. Biol. Chem.*, 1986, **261**, 4229-4238.

41. C. Eckerskorn, W. Mewes, H. Goretzki and F. Lottspeich, *Eur. J. Biochem.*, 1988, **176**, 509-519.

42. M. Howard, H. A. Jurbergs and J. A. Holcombe, *Journal of Analytical Atomic Spectrometry*, 1999, **14**, 1209-1214.

43. C. M. Halliwell and A. E. G. Cass, *Analytical Chemistry*, 2001, **73**, 2476-2483.

44. T. C. Miller and J. A. Holcombe, *J. Hazard. Mater.*, 2001, **83**, 219-236.

Chapter 2: Choosing Internal Standards Based on a Multivariate Analysis Approach with ICP(TOF)MS

2.1 INTRODUCTION

Signal variations that are not representative of concentration changes in inductively coupled plasma mass spectrometry (ICPMS) can be caused by variations in instrument operating conditions and sample matrix. There are a number of procedures an analyst may use to overcome these instabilities, including isotope dilution, standard additions and internal standardization. The cost of isotopically enriched standards and the applicability restrictions on mono-isotopic species can limit the practical utility of isotope dilution. Standard additions can improve accuracy and correct for many matrix effects, but increased sample preparation time and sample size requirements can limit the application of this technique. Internal standardization generally increases precision, and when a nearly "ideal internal standard" is employed, can improve accuracy. With an "ideal internal standard," one can employ calibration curves prepared from simple standard solutions to determine analyte concentrations in complex matrix solutions, thus simplifying sample preparation and quantitation. In ICPMS, internal standards are routinely used to improve precision with hopes of also improving accuracy.

The ideal internal standard for any given analyte is one whose intensity changes are directly proportional to that of the analyte, i.e., the analyte-to-internal standard intensity ratio remains constant for all changes in the sample composition and instrument performance. However, internal standard choice is limited to elements that are initially absent from the sample or whose concentrations remain constant within measurement

uncertainty. This restriction is not trivial in samples with very complex matrices such as environmental and biological specimens. Chen et al. attempted to overcome this issue by utilizing polyatomics from metal-oxides and Ar as internal standards.[1] There are also a number of studies which indicate that one internal standard, such as ^{115}In, can be used to successfully improve the precision for a variety of analytes.[2-4] ^{103}Rh is another internal standard that is frequently used.[5-7] Several studies, however, have addressed the importance of choosing the correct internal standard for each specific analyte[1, 8-10]. These studies attempted to elucidate the characteristics that might allow a priori selection of an internal standard for a given analyte. Thompson et al.[8] determined that both mass and ionization potential should be taken into consideration while Vanhaecke and colleagues[9] suggest that similarities in mass alone are the dominating factor for internal standard choice. A study by Sartoros et al. used cluster analysis to develop an automated system for determining the best internal standard.[10] This algorithm utilized chemical properties such as kinetic energy and electronegativity for determining analyte-internal standard pairs.

The majority of internal standard studies to date have used a quadrupole mass analyzer, which is limited in its multielement capabilities.[11] A smaller data set limits the opportunity for statistical analyses of trends when normal distributions are not present. In short, the quantitative, statistical evaluations of elemental properties that contribute to a good analyte-internal standard pair have been very limited. Although general trends have been determined in the previously cited studies, it is difficult to ascertain the number of and reasons for exceptions that may exist. From the previous work, the extent of the loss

in precision and accuracy that would result from choosing a less than optimal internal standard or using no internal standard is unclear.

In ICPMS there are a large number of parameters that impact the relationship between analyte concentration in a sample and the signal recorded from the detector. They begin with nebulizer efficiency, and proceed through physicochemical processes in the plasma and ion pathways in the optics and spectrometer. Fundamental studies of individual processes continually appear and provide insights that ideally will lead to a master equation, allowing one to predict signal magnitude and dictate the practical selection of the nearly ideal internal standard for any given analyte. However, the complexity and interdependencies of these processes make this noble objective a daunting task.

The present study attempts to cover a diverse set of operating conditions and sample matrices for a large number of elements to generate a database series from which specific predictions and statistical evaluations regarding internal standard selection can be made. Ideally, the information will suggest characteristics of the analyte that will permit *a priori* selection of an internal standard, e.g., similarities in mass, ionization potential, etc. Four different condition sets were evaluated: acetic acid (CH_3COOH) matrices, sodium chloride matrices (NaCl), sample delivery rates to the nebulizer and torch position relative to the sampling cone. The acetic acid matrix (0-10%) simulates a relatively difficult to ionize matrix with a high carbon content. The NaCl matrix (0-500 ppm) emulates a common "salt matrix" with an easily ionizable element. The sample delivery rate perturbations simulate potential nebulizer blockage and other parameters affecting aerosol formation, e.g., solution viscosity, surface tension. The alterations in

torch-to-sampling cone distances simulate variability changes in plasma temperature at the sampling cone, extent of elemental/ion diffusion, electron density at point of plasma sampling, etc.

One goal of the current study is to correlate a variety of elemental properties to the selection of optimal analyte-internal standard pairs. The first step in attempting to establish such a correlation that would permit a priori selection of an analyte-internal standard pair might be to evaluate all elements as potential internal standards for all possible analytes (i.e., all other elements). The simultaneous multielement detection capabilities of a time-of-flight based ICPMS system permit collection of all masses without sacrificing duty cycle for any given m/z being monitored. However, some restrictions are imposed by, for example, intense ion flux from plasma gases (e.g. Ar^+, Ar_2^+, ArO^+, etc.).

The properties considered include mass and ionization potential,[12] various thermodynamic properties of formation,[12] electronegativity,[13] elemental charge in solution and ionic mobility in solution. For example, with an altered temperature or electron density in the plasma, analyte-internal standard similarities in enthalpies or ionization potentials may be parameters worth matching. Similarly, with altered matrices, inter-ionic interactions (e.g., space charge effects) in the interconal regions or in the ion optics are known to exhibit dependencies on mass. Correlations to charge and ionic mobility of the elements in solution were evaluated to determine whether disproportional ionic distribution might exist within the aerosol droplets and alter the signals could have a significant impact on internal standard performance, especially during the experiments in which sample delivery rate to the nebulizer was changed. A

number of studies have addressed this phenomenon known as aerosol ionic redistribution (AIR) and its affect on analyte signal.[14-17] While it might not be possible to elucidate a definitive "rule" for choosing the best internal standard, the present study will show how to isolate and evaluate the efficacy of using general trends as a means of choosing the best internal standard for any given analyte.

Finally, a set of nine analytes with varying physicochemical properties were determined under altered instrumental and matrix conditions using calibration curves prepared from optimized ICPMS operating conditions and simple standards in 1% HNO_3. These data constituted an evaluation series. This second series consists of two separate goals. The first of which is to determine the utility of the original database series as a means of internal standard prediction. Internal standardization was performed on these analytes to determine the impact of internal standard choice on both analytical precision and accuracy. The prediction scheme created for the database series was used to select the internal standard, and these results were compared to the use of alternative internal standards as well as using no internal standard. In making these comparisons, the evaluation series will offer additional insight into the quantitative penalties of using a non-optimal internal standard.

2.2 EXPERIMENTAL PROCEDURE

2.2.1 Instrumentation and Reagents

All data were collected on a GBC Optimass 8000 (GBC Scientific, Hampshire, IL, USA) inductively coupled plasma orthogonal time-of-flight mass spectrometer using

a Meinhardt concentric glass nebulizer and the GBC cyclonic spray chamber. Multi-element and single element standards were combined to make a 10 ppb standard containing 54 elements. Distilled, deionized water and ultra high purity HNO_3 (Fisher Scientific) were used in all cases. Trace metal grade acetic acid (Fisher Scientific) and NaCl (Sigma Chemical Company) were used in matrix laden samples.

2.2.2 Procedure

All glassware was washed in 4 M HNO_3 for at least 24 h and deactivated with 2, 2-dimethyldichlorosilane. Class A polymethylpentene (PMP) volumetric flasks were used for the evaluation series.

The database series was prepared using dilutions of the multielement standards. In all cases, the analytes were present at 10 ppb for all 54 elements. The conditions employed to generate the database values are detailed in Table 2.1. Solutions in 1% HNO_3 were employed to study condition changes in torch position, sample delivery rate and long term drift.

Table 2.1: Experimental design of database series, where one parameter is changed at a time to evaluate its impact on internal standardization of each evaluated analyte.

Condition Name	Matrix	Matrix Conc.	Torch Position (mm)[a]	Sample delivery rate (mL/min)[b]
Sample delivery rate (mL/min)	HNO_3	1%	6	0.6, 0.9, 1.3, 1.6, 1.9, 2.2, 2.5, 2.9, 3.2
Torch Position	HNO_3	1%	6, 7, 8, 9, 10, 11, 12, 13, 14, 15	1.6
NaCl matrix	NaCl	0, 1, 500 ppm	6	1.6
Acetic matrix	CH_3COOH	0, 0.1%, 1%, 10%	6	1.6

These 54 element standards were also made in varying concentrations of glacial acetic acid and NaCl to evaluate the effects of sample matrix on internal standard choice. From Table 2.1 it can be seen that ICPMS intensity information was obtained for 27 different "variations" (including optimized "baseline" runs) within five "conditions". Initially, 224 masses were monitored for each variation, from which 102 m/z values, representing 51 elements, were subjected to detailed data analysis. (Criteria for data set reduction are given below in Data Analysis section.)

An evaluation series was prepared to assess the internal standard selection criteria suggested by the database series results. The evaluation series consisted of nine elements covering a wide range of m/z, and were run at 50 ppb under varied matrix and instrument conditions to evaluate the effect of internal standardization on analytical accuracy and precision. Evaluation was based on the use of simple standards in 1% HNO_3 using optimized instrument settings to prepare a calibration curve for quantitation, independent of the test condition or matrix composition. Instrument settings were adjusted to

optimize the collective signal strengths of 5 elements (Be, Co, In, Pb and Th). The test solutions employed several different perturbed conditions, i.e., sample delivery rate of 0.6 mL/min and 1.9 mL/min; torch positions of 6 and 12 mm; 5% CH_3COOH; and 10 ppm NaCl matrix.

2.2.3 Data Analysis

Initially, 224 masses were monitored and exported for further data analysis. Elimination of masses from the database series were based on: a) an element's absence in the standard, b) low signal due to low isotopic abundance, and c) significant isobaric and Ar^+ or ArX^+ interferences. All isotopes for K were eliminated based on low signal and Ar^+ interferences. All isotopes of Si and Na were eliminated as a result of large background interferences in the blank. This initial data processing left 102 masses from 51 elements for further analysis. The ICPMS produced data for the five standard conditions and 27 variations, yielding useful intensity information for 51 unique elemental-system situations. These were organized in Microsoft Excel with each worksheet containing the intensity ratio of each remaining mass to the 102 m/z values in the set. Thus, 5202 unique ratio values were available per condition. A Microsoft Excel macro written in Visual Basic for Applications (Microsoft Visual Basic 6.3) was used to calculate these ratios from the imported intensity data. This macro was used to calculate the percent relative standard deviation (%RSD) of each ratio through a changing set of conditions for every analyte-internal standard pair. The calculated %RSDs were used in the data analysis as well as in the prediction of good analyte-internal standard pairs.

JMP6 (SAS) was used to calculate correlations and multiple ordinary least squares (OLS) regression equations to establish relationships between analyte-internal standard pairs and a variety of physical and chemical properties.

2.3 RESULTS AND DISCUSSION

2.3.1 RSD of an Internal Standard Ratio as an Indicator of Spread

A small RSD calculated over a range of conditions (e.g., varied NaCl concentrations) suggests that the internal standard signal is changing in proportion to that of the analyte. Thus, a small %RSD should represent a good analyte-internal standard pair. If a correlation between %RSD and chemical property can be found, an *a priori* selection of "ideal" analyte-internal standard pairs may be possible. It should be noted that the data are not normally distributed and the calculated RSD should be viewed as a measure of relative spread of values rather than an actual uncertainty in the data. Using the RSD may not give an accurate assessment of how ideal an internal standard is in cases where only one particular parameter (*e.g.,* an extreme pump speed) caused a large change in the analyte-to-internal standard ratio.

2.3.2 Correlation Plots

Correlations between %RSD and changes in chemical properties were calculated to evaluate the presence of a relationship between good internal standards and similarities in chemical properties. Plots were prepared for each perturbation studied, for each analyte ratioed to all other recorded elements.

As an example, Figure 2.1A shows a strong correlation between internal standard choice and the mass difference between internal standard and analyte, *viz*., a small mass difference between analyte and internal standard correlates to a small %RSD. An example of a very weak correlation is represented in Figure 2.1B where the change in ionization potential exhibits virtually no relationship to %RSD.

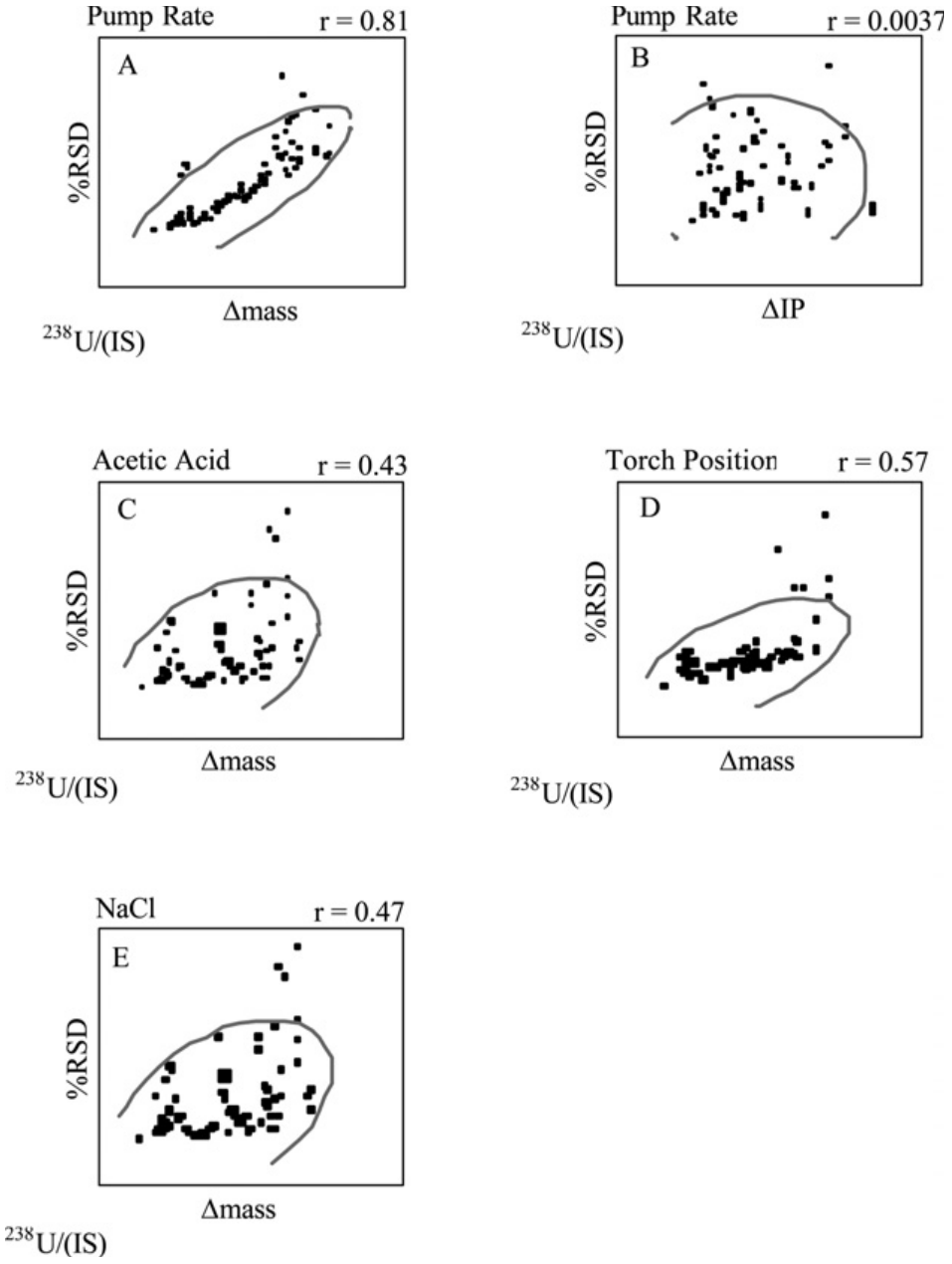

Figure 2.1 A-E. Example correlation scatter plots. Each point represents a ratio of ^{238}U and one of approximately 100 internal standards considered during the specified perturbations. The solid lines are set to encompass 95% of the points.

As expected from the results observed by other authors,[8,9] mass typically offered the strongest correlation to %RSD for every condition. However, as shown in Figure 2.1C-E, the level of correlation with mass for different perturbation sets and different analytes can be highly variable. For the nearly 2,000 correlation plots created, most correlations were not as distinctively differentiated as shown in Figures 2.1A and B, but offered less definitive conclusions such as those data in Figures 2.1C-E. Thus, using well correlated data or outliers (i.e., poorly correlated) to draw general conclusions became difficult primarily because of the continuum of data between good and poor correlations.

2.3.3 Multiple Ordinary Least Squared (OLS) Regressions

While the correlation graphs provided a quick visualization of dependencies, a more quantitative approach was necessary to evaluate the relationships established by the correlation plots. Multiple OLS regressions offered a method that is not only quantitative, but takes the relative relationships between chemical properties into consideration and is unaffected by differences in units. Using the data from all 102 isotopes (51 elements), regression equations were calculated for the most abundant isotope of each element with no interfering isobars. Linearity, homoscedasticity and normality were needed for valid analysis by OLS, and each model was tested for these characteristics. It should be noted, however, that some elements yielded more valid models than others. Normality was the most difficult specification to meet, although some elements did meet this requirement. The elements that did not have a normal distribution among the residuals were approximated as normal by the Central Limit Theorem since n is large. However, the tests for these elements are less predictive than

the tests for elements that did not need to rely on this theorem. Therefore, this method was suitable for general trend analysis within a reasonable margin of error, but probably should not be used for individual predictions. Log-log normalization was used to improve some of these specifications. Quantitative t- and F- tests were used to establish and rank significance among the different chemical properties considered. Four separate regression equations were calculated for each major isotope from the four different perturbations considered. Therefore, a total of 204 equations were calculated using JMP6 (SAS) in the form illustrated in eq. 2.1.

$$Y = \beta_1 x_1 + \beta_2 x_2 + ... + \beta_n x_n \quad (2.1)$$

Y represents a predicted %RSD, x represents a change in chemical property and β is the slope, or proportionality constant, that signifies the relationship between %RSD and each change in chemical property.

The magnitude and standard error of the slope corresponding to each change in chemical property was used as the basis for the significance testing. Both the t- and F-tests work under a null hypothesis of H_0: $\beta = 0$ and an alternative hypothesis of H_1: $\beta \neq 0$. A slope of zero is indicative of no correlation between a given chemical property and %RSD. Significance was defined by a p-value of less than or equal to 0.1.

If two chemical properties were strongly correlated to one another (strong multicollinearity), the property offering a smaller contribution was removed. This removal was necessary because multicollinearity can affect further significance testing. The variance inflation factor (VIF) was used to quantitatively determine which properties were affected. For example, enthalpy of formation is linearly correlated to Gibb's free

energy of formation. Therefore, these two properties have a strong multicollinearity, and one was always dropped based on relative significance.

Although OLS is often utilized for its forecasting capabilities, the equations derived in the present study are limited for a number of reasons. The lack of normal distribution among the residuals in Y that were previously discussed limits the validity of each model and its predictive capabilities. Another limitation lies in the R^2 values, which varied widely and ranged from 0 to 0.7. Although excellent explanatory coverage was not expected, very low R^2- values offer evidence that there are other potential chemical properties and parameters that may play a role and have not been incorporated into this study. R^2 offers a quantitative measure of the improvement in the error sum of squares on Y resulting from the presence of predictors (X). R^2 can be expressed as a percent of this improvement, so if R^2=0.3, it can be said that 30% of the Y-values are explained by the given predictors. Consequently, the forecasting abilities for the study at hand vary widely with respect to both analyte and condition. Multiple OLS does, however, offer a very effective approach for determining the relative importance of each chemical property on all analytes and over all conditions. For a more detailed discussion of multiple OLS regressions with chemical applications, please refer to the papers by Andrade et al.[18] and Leclerc et al.[19]

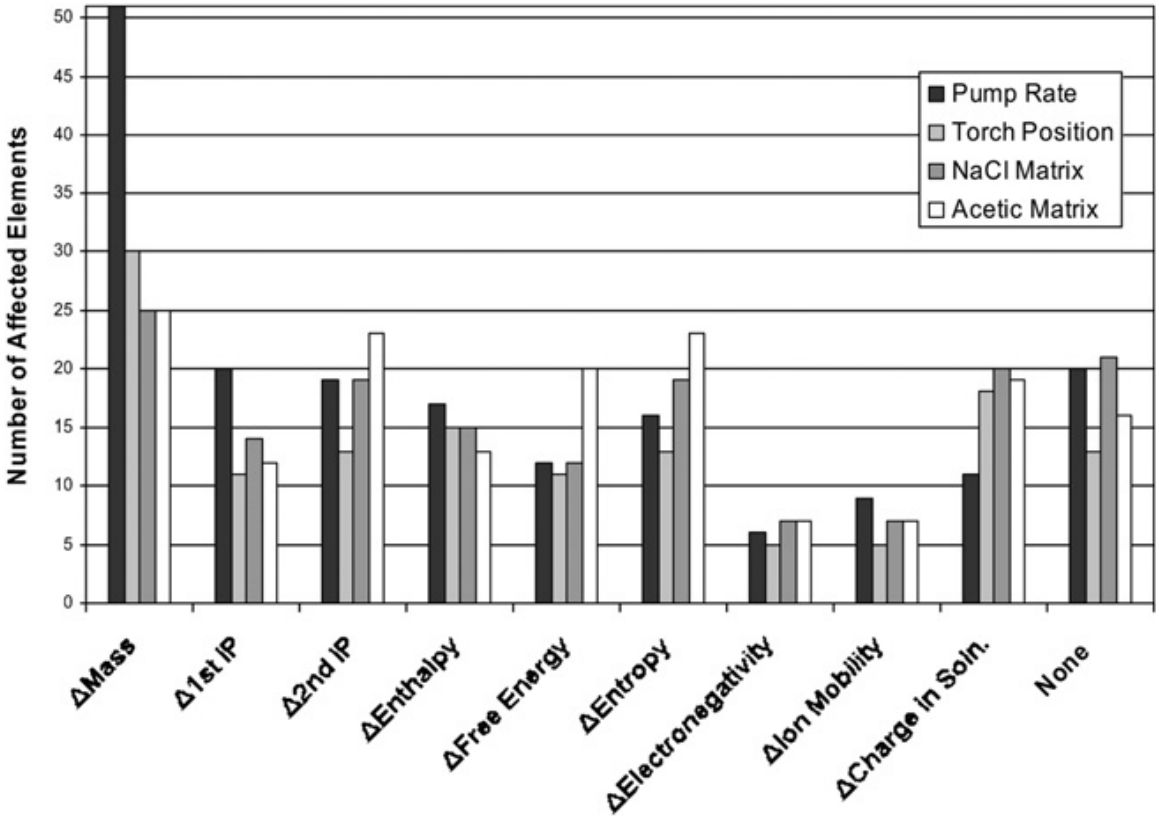

Figure 2.2. The number of elements whose %RSDs are significantly dependent (p-value < 0.1) on each chemical property as determined by a t- or F-test.

As shown by Figure 2.2, mass is the most common predictor for all conditions, especially sample delivery rate. Although a factor for the largest number of elements, mass is not as dominant during other condition changes. For example, internal standard choice in an acetic acid matrix should possibly take 2nd ionization potential and charge into consideration along with mass. This clearly suggests that mass similarity is not the only property that needs to be considered. However, from Figure 2.3, mass is the most significant as well as the most abundant predictor.

Figure 2.2, in contrast to Figure 2.3, is a plot of all the chemical property significances as opposed to the most significant chemical property. Mass shows a greater

dominance in Figure 2.3 for all the conditions represented than it does for Figure 2.2. This implies that although many chemical properties play a role in internal standard compatibility, mass plays a more dominant role in comparison with the other properties considered. The t-scores used to rank chemical properties indicate that for any condition, mass is not only the most abundant predictor, but it is often the strongest. This is especially apparent during the changes in sample introduction rate.

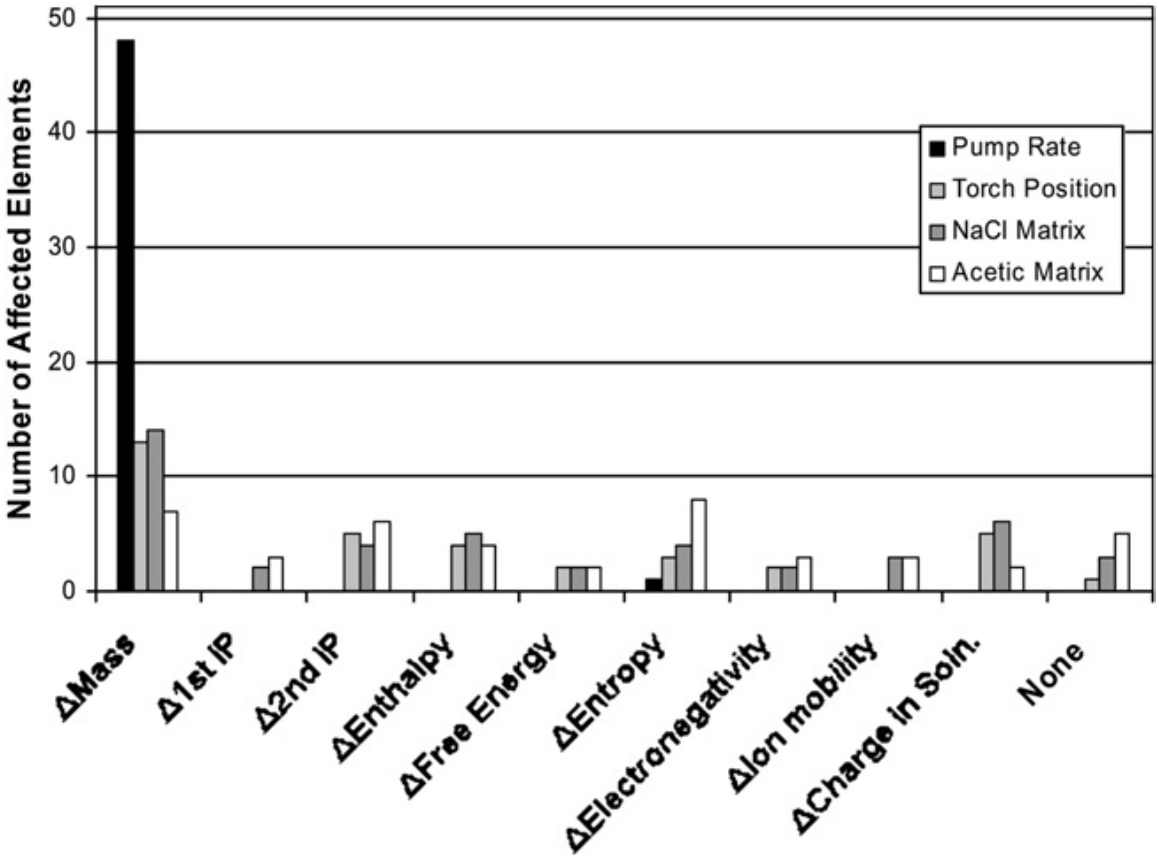

Figure 2.3. The number of elements whose internal standard pairs are most significantly related to each chemical property as determined by the t-values calculated for each model.

The study by Thompson and colleagues[8] concluded that ionization potential was an important factor for internal standard choice. However, the data collected in this study

for 51 pairs indicate that there are only a select few elements that exhibit this dependency for any given condition. Analyte-internal standard pairs that either correlated well or correlated poorly spanned the entire range of ionization potentials, and no single element was dependent on this property for every condition. The change in chemical properties calculated for the purposes of linear regression were absolute. In the case of ionization potential, it may be important to consider the relative values since changes in matrix are expected to impact ionization efficiency.[20] At this time, however, there doesn't seem to be any logical trend as to which elements are significantly affected by ionization potential.

2.3.4 Evaluation of Analytical Accuracy

The nine element evaluation series was analyzed, and the quantitative amounts of each analyte were determined using external calibration curves prepared from simple standards run under optimized instrument parameters as defined in Table 2.2. It should be noted that the slight variations in some of the operating parameters seen between conditions used for the database and evaluation series exist because independent optimization of the ICPMS system was performed before each study. The variations likely reflect the expected interdependencies on many of the adjustable torch and lens parameters and the expectation of arriving at a slightly modified set of optimized conditions.

Table 2.2. Optimized instrument operating parameters.

	Database series	Evaluation series
Sample Introduction time (s)	30.0	30.0
Optimized Sample Sample delivery rate (mL/min)	1.6	1.4
Flush Pump Time (s)	N/A	20.0
Flush Sample delivery rate (mL/min)	N/A	4.8
Acquisition Time (s)	5.000	20.000
Number of Replicates	5	5
Optimized Torch Position X, Y, Z (mm)	6, 0.3, -0.5	8.5, 1.9, 0.2
Nebulizer Gas Flow (L/min)	1.150	0.970
Plasma Gas Flow (L/min)	10.000	11.000
Auxiliary Gas Flow (L/min)	1.000	1.500
Generator Set Power (W)	1300	1200

Table 2.3 shows the analytes and the respective internal standards that were employed for accuracy determination. As noted earlier, the analytes were selected for the diversity of properties represented, e.g., mass, ionization potential, etc. For each condition (torch position, sample delivery rate, 10 ppm NaCl matrix and 5% acetic acid matrix) an internal standard for each analyte was chosen from the database series based on a requirement that they be one of the five internal standard elements showing the lowest %RSD values in the database series. These internal standards will be subsequently referred to as the predicted internal standard for the sake of clarity.

Table 2.3. Analytes and internal standards chosen for their relatively low %RSD for each condition.

	Best Internal Standard from Database Series			
Analyte	Torch Postion	Sample Delivery Rate	NaCl Matrix	CH_3COOH Matrix
^{9}Be	^{7}Li	^{55}Mn	^{121}Sb	^{121}Sb
^{26}Mg	^{55}Mn	^{76}Se	^{44}Ca	^{44}Ca
^{59}Co	^{64}Zn	^{85}Rb	^{121}Sb	^{133}Cs, ^{89}Y
^{115}In	^{109}Ag	^{133}Cs	^{69}Ga	^{166}Er
^{138}Ba	^{152}Sm	^{133}Cs	^{178}Hf	^{88}Sr
^{140}Ce	^{178}Hf	^{153}Eu	^{88}Sr	^{166}Er
^{205}Tl	^{193}Ir	^{193}Ir, ^{178}Hf	^{202}Hg	^{166}Er

It should be noted that often there were more than 5 internal standard elements whose %RSD were sufficiently low to be statistically indistinguishable from the pool of 5 elements from which the predicted internal standard was chosen. This will be expanded on in subsequent sections. To explore the efficacy of using a single internal standard for a range of masses, ^{103}Rh was evaluated as an internal standard for all nine analytes.

All calibration curves exhibited $R^2 \geq 0.999$. Relative error in concentration was calculated based on the differences between the known concentration of each sample and the concentration calculated from the external calibration curves. A statistical t-test was used to determine whether the concentration under the perturbed conditions using the analyte-internal standard ratio and the calibration curve made from simple standards were statistically different from the "true value" of 50 ppb.

The plots in figure 2.4 give the % error for each evaluated analyte-internal standard pair under each condition. Each plot represents the accuracy results for one analyte under all the perturbed conditions. An asterisk (*) above the bar indicates that the there is no statistical difference between the determined and true concentrations. The

error for each analyte include i) using the predicted internal standard, ii) using the predicted internal standard for the other 3 perturbed conditions, iii) using the "universal internal standard" (i.e., ^{103}Rh) and iv) the signal without an internal standard. A wealth of inferences can be drawn from these plots.

^{9}Be has the highest ionization potential of the nine analytes in the evaluation series. In the presence of an acetic acid matrix, all ^{9}Be/internal standard pairs offer worse accuracy than no internal standardization except ^{121}Sb, which is closest to ^{9}Be in ionization potential. However, the use of ^{9}Be/^{121}Sb as an analyte-internal standard pair or no internal standardization for this condition still results in significant analytical error. In the easily ionized NaCl matrix, there is no apparent relationship to ionization potential and all errors were less than 10%, except when using no internal standard. Interestingly, the predicted internal standard, ^{9}Be/^{121}Sb, shows slightly poorer results than the other analyte-internal standard pairs tested in this NaCl matrix.

Using any internal standard was better than no internal standard for altered sample delivery rates in nearly all cases. This is reasonable since it would be expected that any change that primarily affects the amount or size distribution of transportable aerosol would affect all elements similarly. However, the two lightest elements showed exception to this observation, but the cause is unknown at this time.

There are a number of circumstances in which the database series did not isolate the best internal standard. However, in most of these situations the predicted internal standard still provided relatively good accuracy. In the NaCl matrix, for example, the predicted ^{208}Pb/^{114}Cd and ^{115}In/^{69}Ga pairs yielded concentrations that were not statistically different from the true concentration. The same held true for the predicted

$^{140}Ce/^{178}Hf$ pair during a torch perturbation. The finite level of uncertainty due to counting statistics offers an explanation for many such cases, especially where low RSDs were observed, *e.g.*, sample delivery rate variations.

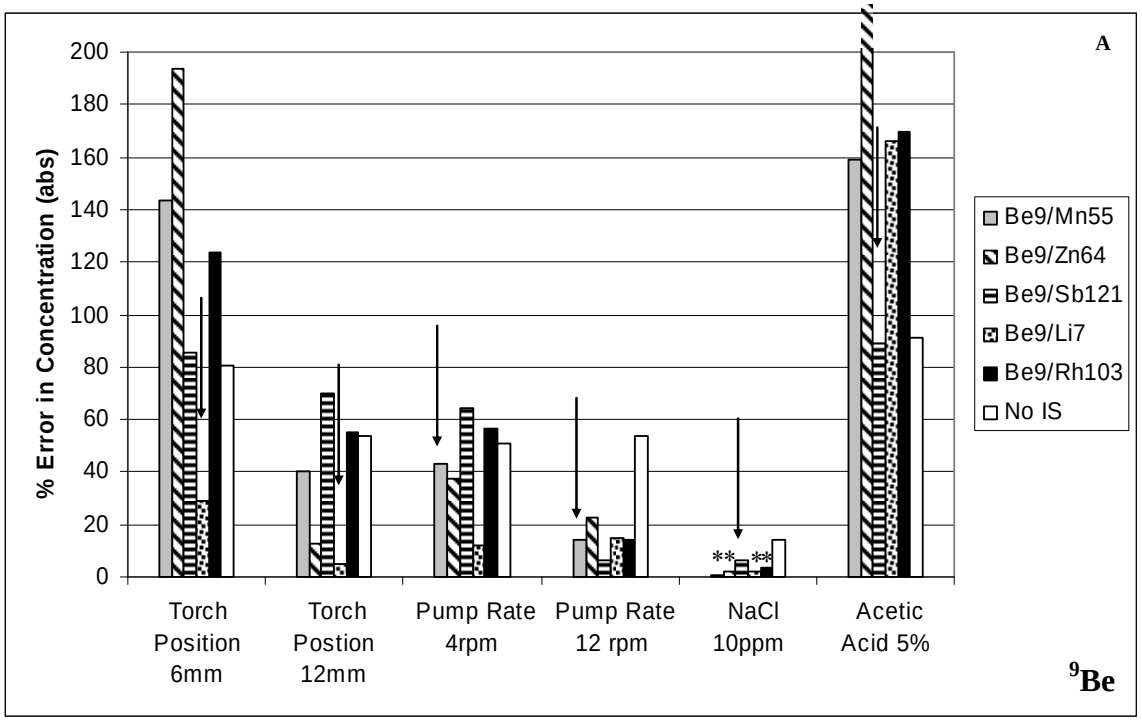

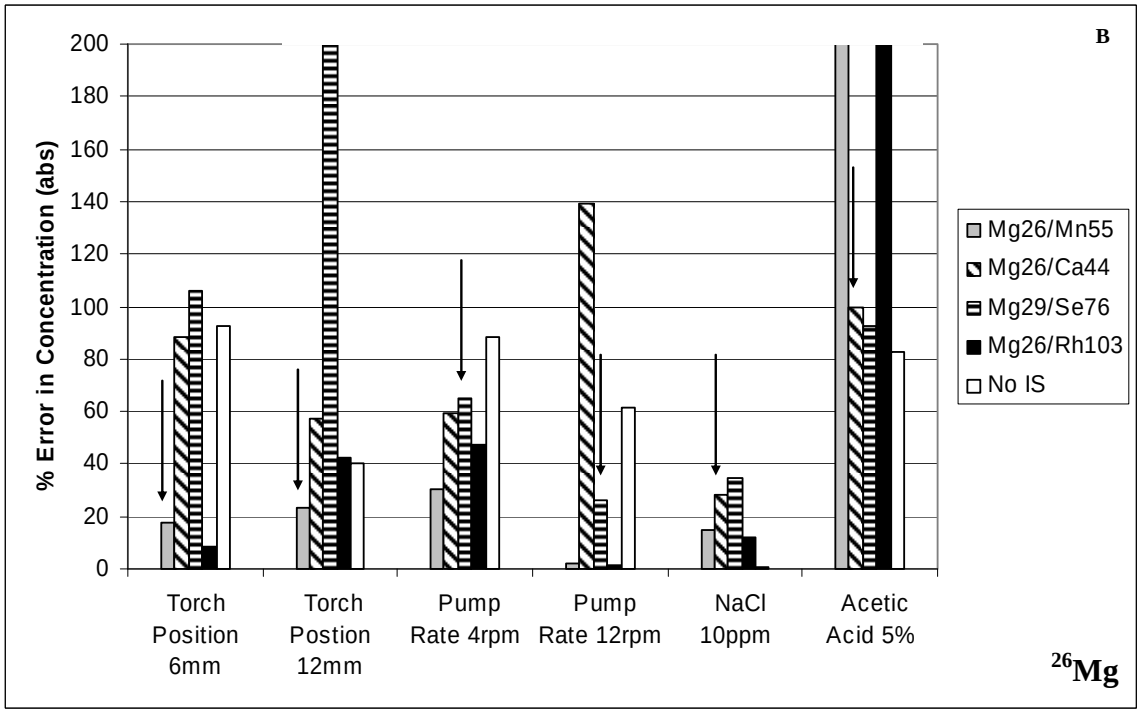

Figure 2.4 (A-B). Please see page 50 for a detailed figure caption.

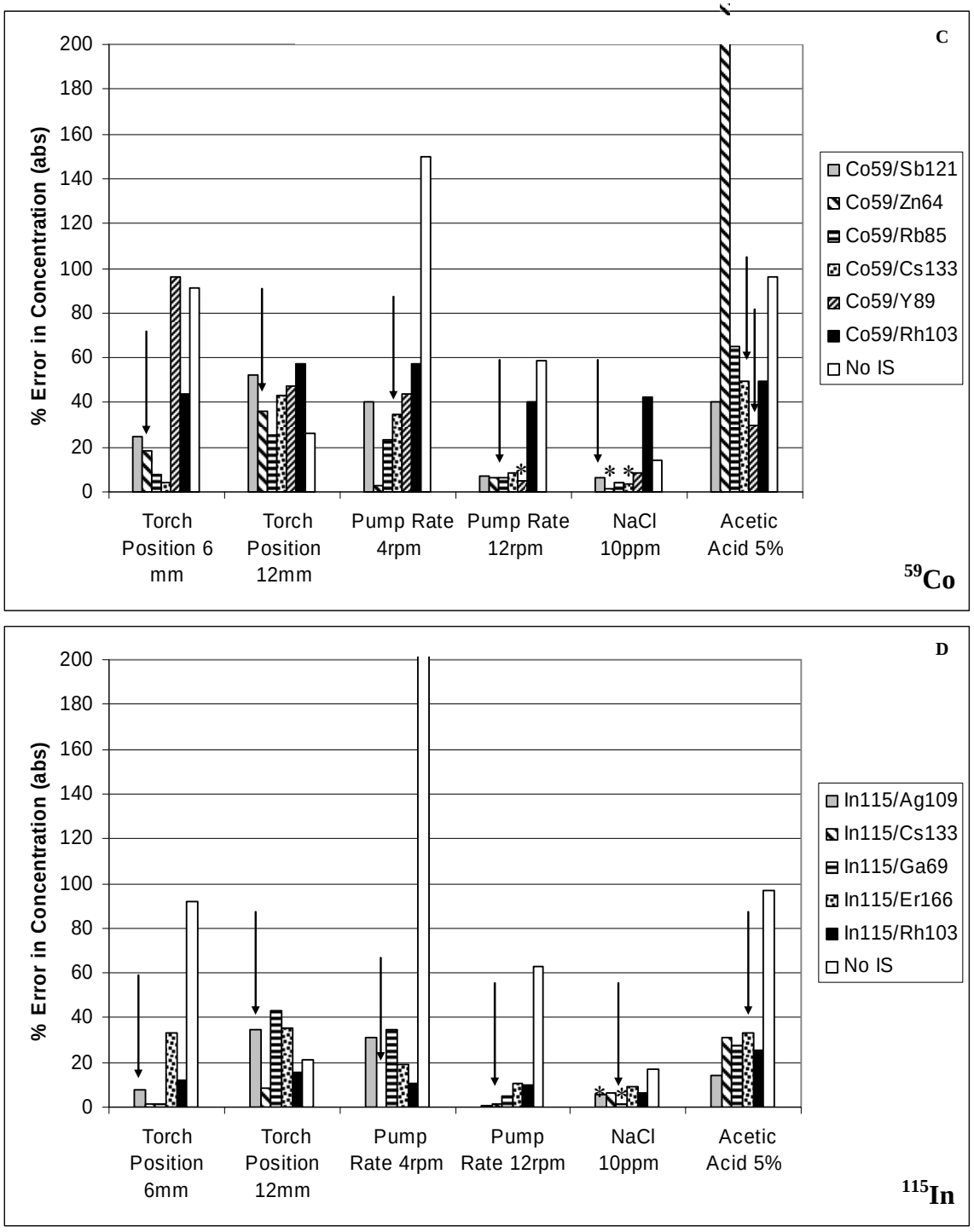

Figure 2.4 (C-D). Please see page 50 for a detailed figure caption.

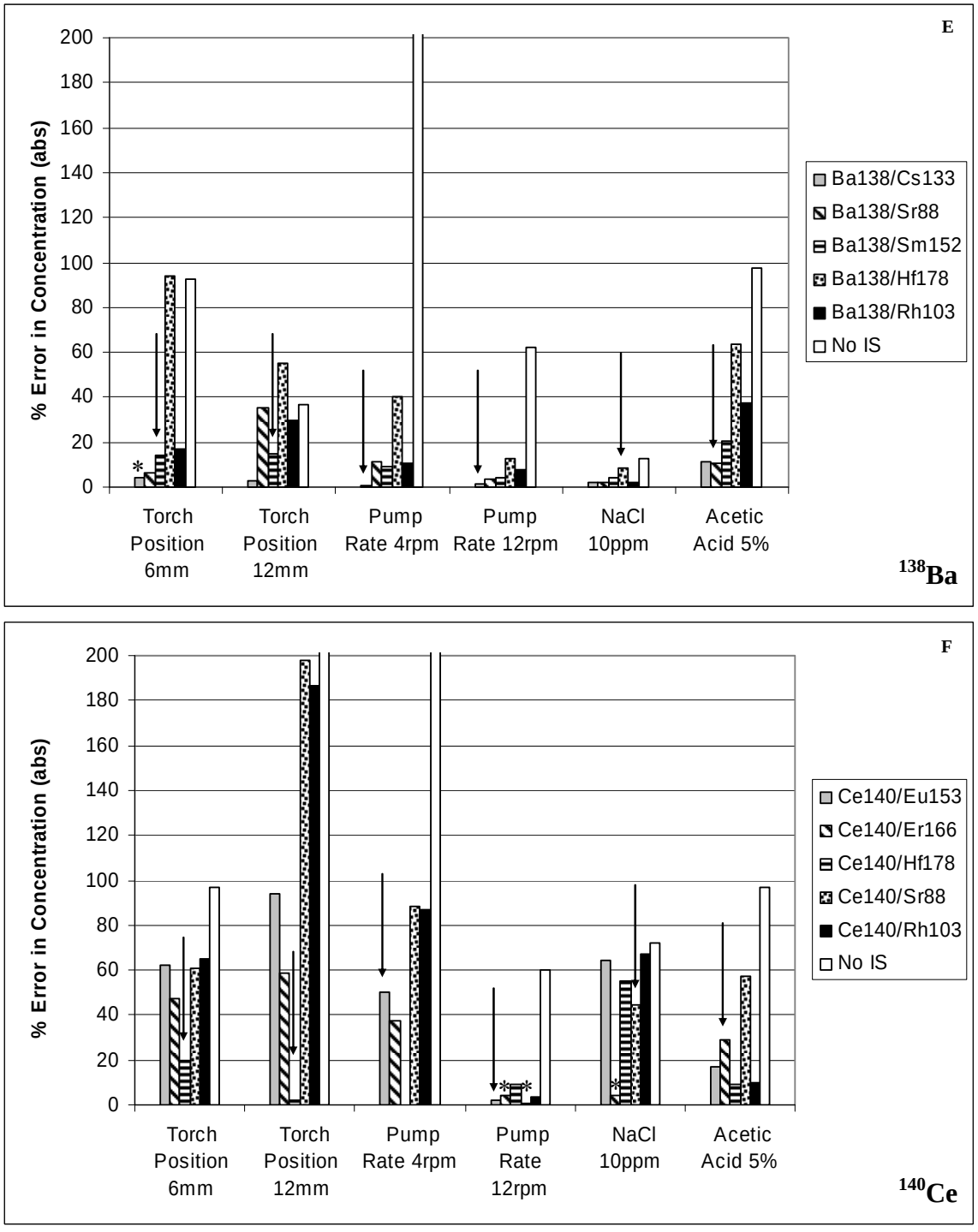

Figure 2.4 (E-F). Please see page 50 for a detailed figure caption.

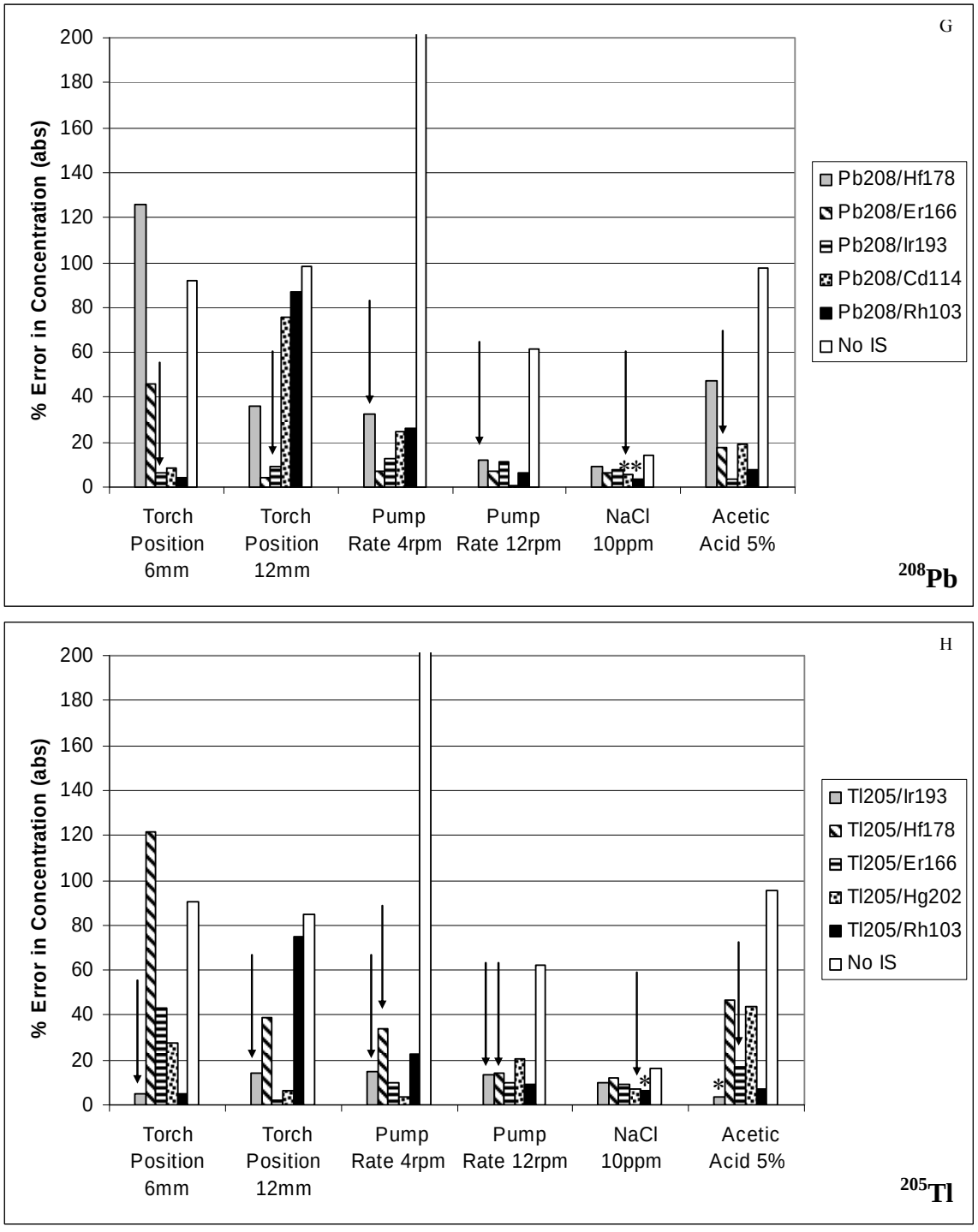

Figure 2.4 (G-H). Please see page 50 for a detailed figure caption.

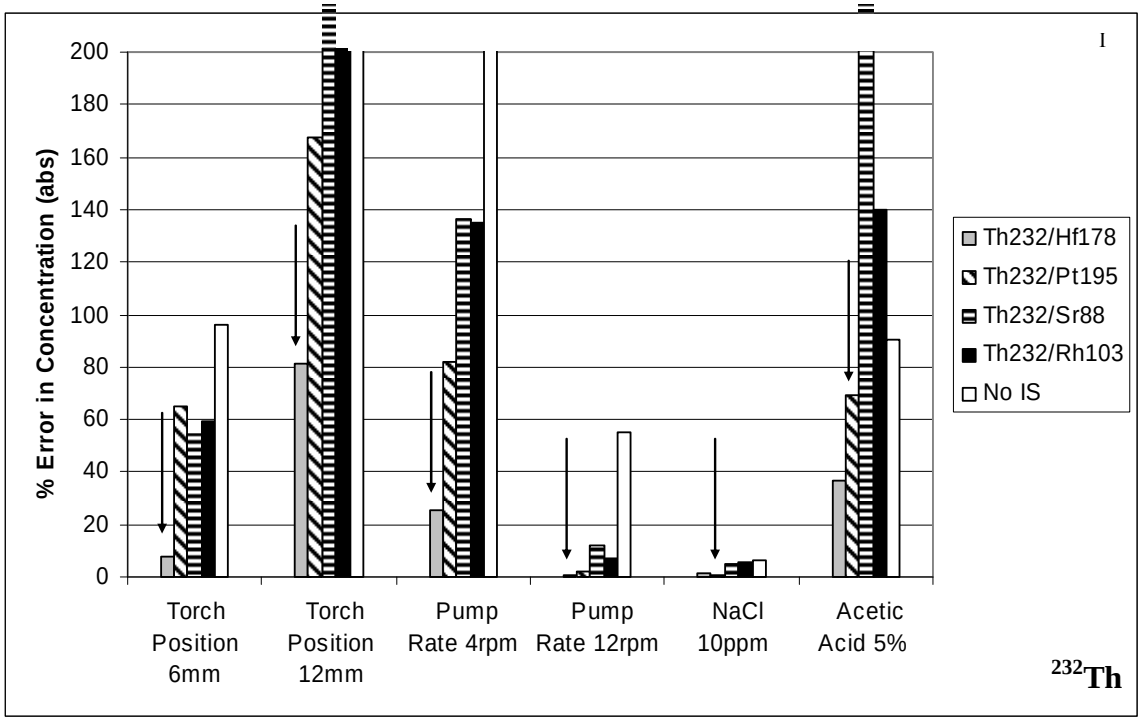

Figure 2.4 (A-I). Evaluation of analytical accuracy measured with relative % error in concentration from the "true value" of 50 ppb. Each bar represents the absolute errors associated with the use of each respective internal standard considered. The arrow indicates the results from a good, general internal standard choice as predicted by the *database series*. The errors associated with ^{103}Rh (as a "universal internal standard") and no internal standard are denoted by black and white error bars, respectively. Asterisks indicate determined concentration that were not statistically significantly different from the "true value." Each of the nine analytes is depicted in a separate plot.

Table 2.4 summarizes which deviations from the database series predictions for the evaluation series can be explained by counting statistics. There are some cases in which the internal standard yielding the lowest % error follows an OLS trend previously discussed. For example, in the torch position condition for ^{138}Ba, ^{152}Sm was predicted to be the best internal standard by the database series. However, for both torch positions considered, ^{133}Cs offers the lowest error, which follows the expected mass trend for ^{138}Ba

under perturbed torch positions. Although similarities in mass seem to correlate to a good analyte-internal standard pair, the data from this series would indicate that choosing the closest mass is not always the best choice. In fact, the results from this study indicate that only approximately 30% of the best performing analyte-internal standard pairs were also those that were closest in mass.

Table 2.4. Summary of pairs where the analytical errors fall within what might be expected from statistical (counting) uncertainties. In cases where the predicted internal standard gave the most accurate result are noted by "—". The blank cells showed less than optimal accuracy with the predicted internal standard but fell outside of accepted precision limits based on counting statistics.

	Internal Standard Discrepancies Explained by Counting Statistics			
Analyte	Torch	Pump	NaCl	Acetic Acid
^{9}Be	--	^{7}Li, ^{64}Zn, ^{121}Sb	^{7}Li, ^{103}Rh	--
^{26}Mg	^{103}Rh	^{55}Mn		
^{59}Co			^{85}Rb, ^{133}Cs	--
^{115}In	^{69}Ga	--	--	^{133}Cs
^{138}Ba	^{88}Sr, ^{133}Cs	--		--
^{140}Ce	--	^{166}Er		
^{205}Tl		^{166}Er, ^{202}Hg		
^{208}Pb		^{166}Er, ^{193}Ir		
^{232}Th	--	--		

In some cases it is possible that the wide range of values for any given perturbation (*e.g.*, NaCl proceeding from 0-500ppm) yielded a prohibitively high dispersion (%RSD); but for any individual perturbation value, there was very little difference. For example, it is conceivable that one element works better than any other as an internal standard over a large range of NaCl concentrations, but it may not be the best internal standard in the 10ppm NaCl matrix, which is the specific matrix tested in the evaluation series. Since Table 2.4 shows that the matrix condition discrepancies are less completely explained by

the uncertainties resulting from counting statistics, it is possible that matrix perturbations are more sensitive to the fact that the evaluation series was collected with a single perturbation value as opposed to a range. Finally, as previously mentioned, there may be uncertainty in the %RSD calculations due to the non-normal distribution of the data.

Some analysts choose to internal standardize with a single element for all analytes. This practice has been evaluated for the current study with ^{103}Rh. In the majority of cases presented, the use of any internal standard gave a more accurate result than when no internal standard was used. However, in approximately 18% of the samples use of ^{103}Rh showed a greater error than when no internal standard was used; and in 33% of the samples, at least one of the internal standard choices led to a larger error than was observed without any internal standard.

It should also be noted that some conditions gave consistently better accuracies than others (e.g., NaCl matrix). Although a 10 ppm NaCl matrix did not appear to create any significant analytical problem, it is clear from the high %RSDs seen in the database series that larger concentrations of NaCl greatly deteriorate analytical accuracies.

2.3.5 Evaluation of Analytical Precision

In many analytical techniques, the use of just about any internal standard should improve analytical precision by compensating for multiplicative enhancements/depressions, *e.g.,* variability of sample volume injected into a GC, slight variations in sample delivery rate to the ICP, etc. An F-test was used to compare the precisions of the analyte signal in the evaluation series with the precision when an internal standard was employed. The results indicated that any time there was a

statistically significant precision difference, the use of an internal standard improved the precision. Some experimental or matrix condition sets saw as much as an order of magnitude improvement in precision from using internal standardization. In only ~35% of the samples, the internal standard that gave the highest accuracy also gave the highest precision for a given analyte. It is possible that there may be different internal standard characteristics that should be considered when high precision is needed over high accuracy. This, however, must be evaluated further.

2.4 CONCLUSIONS

Although many elements show an internal standard choice based on properties other than mass, no other single property stands out among the OLS trends to the same extent. Therefore, minimizing mass differences between an analyte and its internal standard is important, especially in the case of variability in sample delivery rate, as simulated in this study by "pump speed" changes. In an analytical situation, such altered delivery rates may result from partial blockage of nebulizer, peristaltic pump roller noise and possible changes between calibration standards and unknown solution viscosities, surface tensions, etc.

However, similarity of mass between analyte and internal standard is not the only property that should be taken into consideration since there were many situations where the internal standard with a mass closest to the analyte was not necessarily the most ideal internal standard. For example, carbon content as simulated using an "acetic acid matrix" seems to also rely on closeness of the 2nd ionization potential between analyte and internal standard for several elements, although the explanation for such a correlation is

not understood at this time. When it comes to determination of the ideal internal standard for a given analyte, these other properties may become important. As seen in the evaluation data set where simple standards were used for quantitation, the pairs that were closest in mass yielded the most accurate determination in only 30% of the samples analyzed. During the evaluation of analytical accuracy, it became clear that a judicious choice of internal standard can make a significant difference in the validity of concentration measurements. Although most of the results examining accuracy indicated that choosing any internal standard was more effective than calibrating with no internal standardization, a poor internal standard choice yielded analytical errors in excess of 100% in a number of cases.

In all cases, precision was generally improved using internal standardization and no loss in precision was observed in any case. Interestingly, the largest improvements in precision showed little correlation to the best internal standard that would be selected from the evaluation series.

In practice, the method used for collecting the database series is an effective approach for determining the best internal standard if the matrix or other conditions within the sample are unknown or extremely varied from sample to sample. While the best performing internal standard in the nine element evaluation series was not always the internal standard predicted from the database series, the database series prediction generally exhibited relatively little analytical error. If matrix conditions between samples are expected to be less varied and instrument operation relatively stable then it may be prudent to run a short experiment similar to the method used in collection of the

evaluation series data for analytes of interest under the conditions that are expected to dominate signal instability.

It should also be noted that all the data presented were collected from one instrument with one torch and spectrometer design. Some trends (*e.g.*, sample delivery rate's relationship to mass) are expected to be reproducible on other instruments. However, those signal fluctuations that are more dependent on torch design and/or ion optics may result in alternative specific internal standard recommendations. Such potential variability from one instrument to another remains be determined.

It was hoped that one of the outcomes of this study would be the isolation of a small number of physical or chemical characteristics common to analyte and a good internal standard could be used as predictors for internal standard selection. Similarly, isolation of parameters whose difference precluded the use of certain pairs would have been nearly as useful. While the study shows that similarities in mass are common to a large number of good analyte-internal standard pairs, there are a sufficiently large number of exceptions to this "rule" that it should be used with skepticism. These data my serve as a foundation to evaluate trends for a given analyte with respect to designing "rules" or an equation to yield a "quality factor" for potential internal standards for that specific element. However, this element-by-element detailing was not within the scope of this paper.

2.5 ACKNOWLEDGEMENTS

This work was supported in part by the Robert A. Welch Foundation and assistance from GBC Scientific.

2.6 REFERENCES

1. X. Chen and R. S. Houk, *Journal of Analytical Atomic Spectrometry*, 1995, **10**, 837-841.

2. C. Vandecasteele, M. Nagels, H. Vanhoe and R. Dams, *Analytica Chimica Acta*, 1988, **211**, 91-98.

3. J. Wang, W. L. Shen, B. S. Sheppard, E. H. Evans, J. A. Caruso and F. L. Fricke, *Journal of Analytical Atomic Spectrometry*, 1990, **5**, 445-449.

4. J. Wang, E. H. Evans and J. A. Caruso, *Journal of Analytical Atomic Spectrometry*, 1991, **6**, 605-608.

5. M. Y. Perez-Jordan, J. Soldevila, A. Salvador, A. Pastor and M. de la Guardia, *Journal of Analytical Atomic Spectrometry*, 1999, **14**, 33-39.

6. J. Dombovari, J. S. Becker, A. J. Kuhn and W. H. Schroder, 2000, 79-89.

7. M. Wang, *Yejin Fenxi*, 2004, **24**, 19-22.

8. J. J. Thompson and R. S. Houk, *Applied Spectroscopy*, 1987, **41**, 801-806.

9. F. Vanhaecke, H. Vanhoe, R. Dams and C. Vandecasteele, *Talanta*, 1992, **39**, 737-742.

10. C. Sartoros and E. D. Salin, *Spectrochimica Acta, Part B: Atomic Spectroscopy*, 1999, **54B**, 1557-1571.

11. M. Vazquez Pelaez, J. M. Costa-Fernandez and A. Sanz-Medel, *Journal of Analytical Atomic Spectrometry*, 2002, **17**, 950-957.

12. Anon, *CRC Handbook of Chemistry and Physics, 88th ed edited by David R. Lide*, 2008.

13. A. L. Allred and E. G. Rochow, *Journal of Inorganic and Nuclear Chemistry*, 1958, **5**, 264-268.

14. J. A. Borowiec, A. W. Boorn, J. H. Dillard, M. S. Cresser, R. F. Browner and M. J. Matteson, *Analytical Chemistry*, 1980, **52**, 1054-1059.

15. R. K. Skogerboe and S. J. Freeland, *Applied Spectroscopy*, 1985, **39**, 925-930.

16. R. K. Skogerboe and S. J. Freeland, *Applied Spectroscopy*, 1985, **39**, 920-925.

17. Q. Xu, G. Mattu and G. R. Agnes, *Applied Spectroscopy*, 1999, **53**, 965-973.

18. J. M. Andrade, M. J. Cal-Prieto, M. P. Gomez-Carracedo, A. Carlosena and D. Prada, *Journal of Analytical Atomic Spectrometry*, 2008, **23**, 15-28.

19. G. Leclerc and J. J. Pireaux, *Journal of Electron Spectroscopy and Related Phenomena*, 1995, **71**, 179-190.

20. S. H. Tan and G. Horlick, *Journal of Analytical Atomic Spectrometry*, 1987, **2**, 745-763.

Chapter 3: Evaluations of Internal Standard Predictions Across Instrumental Platforms in Inductively Coupled Plasma Mass Spectrometry

3.1 INTRODUCTION

Due to signal aberrations from both matrix effects and instrumental deviations (*i.e.*, plasma flicker) in an inductively coupled plasma mass spectrometer (ICPMS), corrections must be made to achieve accurate and precise results. Three of the most commonly practiced corrections include standard additions, isotope dilutions and internal standardization. Standard additions can be used to correct for matrix effects, but they are generally more time-consuming and do not correct for instrument drift. Isotope dilutions effectively improve both accuracy and precision but can be cost prohibitive when analyzing a large number of elements and are not applicable for the correction of monoisotopic species such as As and Co. Internal standardization is ideally capable of improving both precision and accuracy and can potentially overcome the shortcomings of the two alternative methods. It employs a relatively simple sample preparation that utilizes external calibration standards and samples that are all spiked with the internal standard (IS) to be used. Calibration curves are then constructed with the analyte/IS ratios on the ordinate. The difficulty of this technique lies in choosing an internal standard. The ideal internal standard must meet two equally important requirements: it must not be present in the original samples in varying amounts, and its signal magnitude must change exactly proportionally to that of the analyte regardless of system perturbations. Upon meeting these two requirements, any changes to the analyte/IS ratio is solely reflective of a change in analyte concentration. Fulfillment of the second requirement will be the focus of the present study. To achieve this proportional change in signal magnitude, the analyte and IS must be affected by system perturbations, such as

changes in sample introduction rate, in exactly the same way. Therefore, it is expected that the elements must share some key properties, and an understanding of which properties are important would allow *a priori* selection of the ideal internal standard. To date, there is no mathematical relationship that predicts signal magnitude based on some fundamental knowledge of analyte, matrix or instrument properties. However, many studies suggest that similarity in mass between analyte and IS is important, if not the most important factor that need be considered.[1-3] Ionization potential[1] and other properties[3] have also been found to play a role. Conversely, some analysts choose a single internal standard such as ^{115}In[4-6] or ^{103}Rh[7-9] to improve precision for all analytes.

In a previous study, a prediction scheme was developed based on the idea that taking the RSDs of analyte/IS ratios over a set of system perturbations would effectively allow an analyst to rank IS performance.[10] Because the program outputs a ranked list, it is often possible to choose from a group of relatively good internal standards. This feature offers flexibility insofar that an analyst can choose an internal standard based on performance, sample background and any other number of desired features. To create this prediction scheme, over 5,000 unique analyte/IS pairs were monitored through 37 system perturbations. RSDs from the prediction data and a variety of chemical properties were used to develop multiple ordinary least squares (OLS) models that could elucidate which chemical properties were most important to internal standard performance under varying system perturbations. Mass was overwhelmingly found to be the most imperative property in predicting a good analyte/IS pair. That being said, it was by no means a universally reliable criteria, and there were a multitude of exceptions. The practical utility of the prediction scheme was determined with an evaluation experiment. Nine analytes over a wide range of masses and other chemical properties were monitored using one of their optimal internal standards as predicted earlier. A simple calibration

curve was constructed and "samples" were evaluated under different perturbations. All samples contained metal concentrations at 50 ppb. Analyte concentrations were calculated along with the errors in concentration. The results were promising with predicted analyte/IS pairs often offering the lowest error. These results also emphasized the importance of choosing a good internal standard since there were cases which illustrated a poor internal standard choice yielding larger errors than using no internal standard. ^{103}Rh was used to evaluate the efficacy of using a single internal standard for all analytes. Although interesting, the performance of this prediction scheme had yet to be tested over a long period of time or on a different instrument. Therefore, its utility in a practical sense remained in question. The present study seeks to recreate the evaluation series of Finley-Jones et al. [10] on the same instrument after extended use, including many re-optimizations, and on a completely different ICPMS system to determine the validity of using the original prediction scheme without the large-scale data collection required for this program. Similarities and differences between data sets may offer insight into analyte/IS performance.

3.2 EXPERIMENTAL PROCEDURE

3.2.1 Instrumentation and Reagents

Data for GBC 1 and 2 were collected on a GBC Optimass 8000 (GBC Scientific, Hampshire, IL, USA) inductively coupled plasma orthogonal time-of-flight mass spectrometer using a Meinhardt concentric glass nebulizer and the GBC water cooled cyclonic spray chamber. Agilent data was collected on an Agilent 7500cx (Agilent Technologies, Foster City, CA) inductively coupled plasma quadrupole mass spectrometer and a micro-mist nebulizer with an Agilent polypropylene spray chamber. Multi-element and single element standards were combined to make standards and

samples containing 39 elements. Distilled, deionized water and ultra high purity HNO_3 (Fisher Scientific) were used in all cases. Trace metal grade acetic acid (Fisher Scientific) and NaCl (Sigma Chemical Company) were used in samples where the matrix was altered. Table 3.1 lists the optimization parameters used for each data set.

Table 3.1. Optimzation parameters for each data set.

	GBC 1	GBC 2	Agilent
Sample Introduction Time	30.0	30	20
Optimized Sample Delivery Rate (mL/min)	1.4	1.6	0.96
Flush Pump Time (s)	20.0	20.0	30.0
Flush Sample Delivery Rate (mL/min)	4.8	4.8	4.7
Acquisition Time	20.000	20.000	26.3333
Number of Replicates	5	3	3
Optimized Torch Position X, Y, Z (mm)	8.5, 1.9, 0.2	7.5, 2.0, 0.7	8,-0.3, 0.4
Nebulizer Gas Flow (L/min)	0.970	1.060	0.95
Plasma Gas Flow (L/min)	11.000	11.000	
Auxiliary Gas Flow (L/min)	1.500	1.400	0.21 (make up gas)
Generator Set Power (W)	1200	1050	1500

3.2.2 Sample Preparation

Class A polymethylpentane (PMP) volumetric flasks were used for the preparation of all standards and samples. A calibration curve was prepared by varying

the concentration of 9 analyte elements (10-100 ppb) and holding the remaining 30 elements at 50 ppb to act as internal standards. Table 3.2 lists the internal standards used for each perturbation as predicted in.[10]

Table 3.2. Internal standards predicted in Finley-Jones et al.[10] for each perturbation. Multiple predictions indicate that the RSDs were not statistically different within the original prediction scheme.

Analyte	Torch Postion	Pump Speed	NaCl Matrix	Acetic Acid Matrix
Be	Li	Mn	Sb, Li	Zn, Sb
Mg	Mn	Se	Ca	Ca
Co	Zn	Rb	Sb	Cs, Y
In	Ag	Cs, Ag, Rh	Ga	Er
Ba	Sm, Rh, Sr, Cs	Cs, Rh, Sm	Hf	Sr
Ce	Hf	Eu	Sr	Er
Pb	Ir, Er	Hf	Cd	Er
Tl	Ir	Ir, Hf	Hg	Er
Th	Hf	Hf	Sr	Pt

The calibration curves were run using instrument settings optimized for maximum sensitivity and a matrix of 1% HNO_3. Samples to be quantified consisted of a number of system perturbations including an alteration of sample introduction rate, torch distance from the sampling cone and two different matrices. The sample introduction rate was changed by altering the pump speed of the peristaltic pump. It should be noted that a faster pump rate was used in GBC 2 and the Agilent in response to the increased optimized pump rates determined. The sample introduction and the torch position perturbations were run using the 50 ppb calibration standard. The matrix perturbations were made with all elements at 50 ppb in 10 ppm NaCl for GBC 1, 100 ppm NaCl for GBC 2 and the Agilent, or 10% CH_3COOH for all three data sets.

3.2.3 Data Analysis

Predicted internal standards were chosen based on the procedure outlined by the previous study [10]. Analyte/IS ratios were calculated and used to plot calibration curves for each of the nine analytes. All calibration curves exhibited r^2 values of >0.999. These calibration curves were used to calculate the analyte concentrations of each perturbed sample previously described. Error in concentration was calculated by using the relative difference between the calculated concentration and 50 ppb. This error was used to compare different internal standards and the use of no internal standard. Statistical t-tests were used to determine whether the errors were statistically significant and to compare errors between different analyte/IS pairs.

3.3 RESULTS AND DISCUSSION

3.3.1 Long Term Utility of Prediction Scheme Data Set

It is important to determine whether the internal standards predicted in the previous study[10] are still valid despite the passage of time and inevitable instrument re-optimizations. The goal is to determine whether it is necessary to collect prediction data on a regular basis or whether a single collection will suffice, *i.e.*, have long term utility. Two data sets, taken over six months apart, were compared for the present study. Not only did multiple re-optimizations take place within this six month period, but the torch was replaced and the nebulizer was repaired; all of which could significantly impact analyte/IS performance. Table 3.1 summarizes the operating parameters used for each data set. The results of GBC 1 were reported extensively in the previous study.[10]

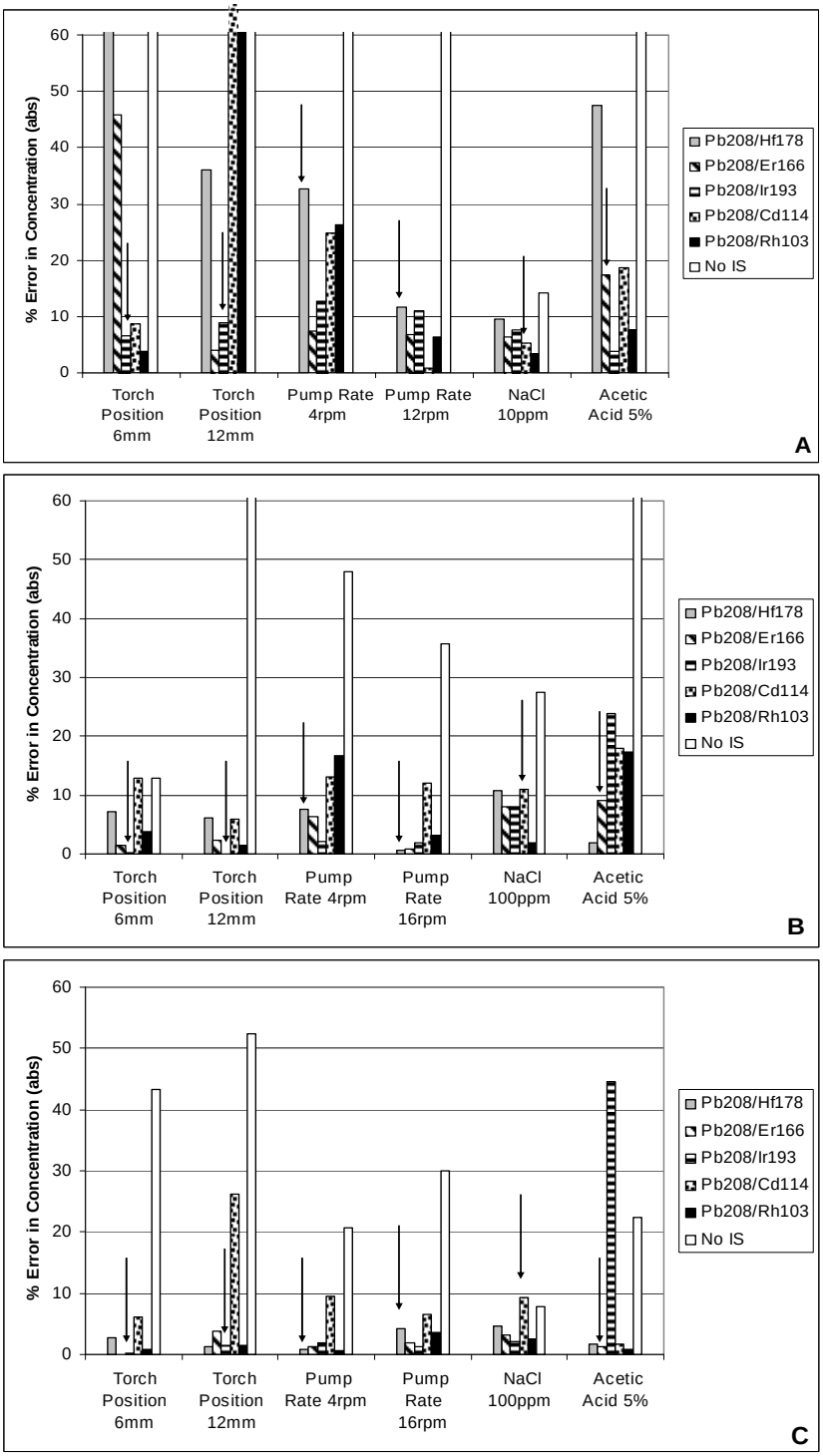

Figure 3.1. Error plots of GBC 1 (A), GBC 2 (B) and the Agilent (C) system with Pb as the analyte to illustrate some general trends. Arrows indicate the analyte/internal standard pair that was predicted as optimal.

Figure 3.1 A-C plots the results for Pb (analyte) and several internal standards for the different perturbations that were chosen based on the prediction scheme proposed in the previous study.[10] It should be noted that Figure 3.1 acts as a representative illustration of the general trends observed in a majority of analytes evaluated. The absolute error in concentration on the ordinate is shown for various perturbation parameters with each bar representing the error from a given analyte/IS ratio. An arrow indicates the IS that was predicted by the previous study to perform as an optimal internal standard. From these plots, it is clear that GBC 2 produced lower errors than GBC 1 even though the data were collected on the same instrument. This trend was seen throughout the majority of analytes considered. Since the analyte signal magnitude at most perturbations were similar between the two sets, the lower errors of GBC 2 cannot be attributed to a plasma that is less susceptible to changes in the absolute signal magnitude. Although signal magnitude does not vary to a great extent between the two data sets, it does change significantly within both, thereby stressing the important role played by internal standarization.

Despite differences in the magnitude of concentration error, many of the relative trends with respect to internal standard prediction remain consistent in these two data sets. It would be unreasonable to expect identical error trends due to the multitude of changes in operating parameters and the inevitable aging of instrument components.

3.3.2 Analysis of Internal Standard Performance on Two Different Instruments

Besides the obvious difference in mass analyzers between the two instruments (viz., TOF vs quadrupole), there are other variations that must not be overlooked. It is

very likely that differences in the nebulizer, spray chamber, torch design and tuning parameters may also impact signal trends and internal standard performance. Therefore, it becomes difficult to assign specific instrumental factors to variations in performance. An example error plot for the Agilent can be seen in Figure 3.1C. Errors on the Agilent were generally lower than both GBC 1 or 2. It is important to note that these lower errors are not a consequence of the analyte signal showing smaller changes with different perturbations. This is evidenced by the similar error magnitudes calculated for both the GBC and the Agilent when no internal standard was used. Thus, internal standardization seems to be generally more effective with the instrument used in collecting Agilent data.

Figure 3.2 represents the number of internal standards that were correctly predicted based on the prediction scheme described previously[10] for each perturbation listed.

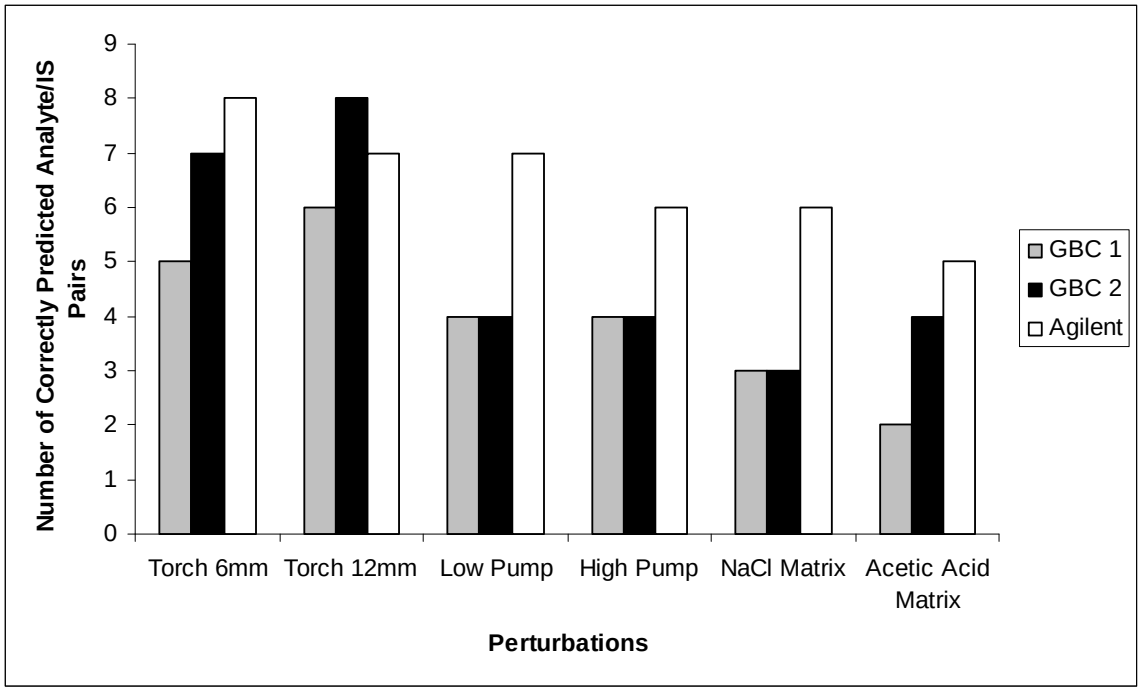

Figure 3.2. Number of correctly predicted analyte/IS pairs for all three data sets.

When the predictive data from the GBC system was applied to the Agilent system; rather than finding completely different internal standard trends for a given analyte, the predicted internal standard actually yielded the most accurate results for the Agilent. In fact, for the Agilent a number of the internal standard selections provided errors that were low and not statistically different from the performance of the predicted internal standard.

Although data from the Agilent appeared to offer lower error overall, the errors resulting from the predicted internal standards from GBC 2 and even GBC 1 were often equally low. It would be unreasonable to expect the relative patterns in error to be identical when considering all of the experimental variables that have changed from one instrument to the next, yet there are cases in which they were remarkably similar. For

example, in Figure 3.1B and C at the 6 mm torch and NaCl matrix perturbations, the relative error trends of all the elements correlate very well.

However, there were some perturbations that differed when the two different instruments were compared. For example, the acetic acid matrix does not produce nearly as large a signal suppression for analyte and internal standards in the Agilent. Because of the carbon and molecular load placed on the torch, it is possible that a combination of torch/coil design and/or nebulizer/spray chamber performance are the primary causes of the larger signals for the metal ions in the Agilent.

A representative scatter plot comparing the error of the predicted IS, the use of Rh as the IS for all analytes and the use of no IS for GBC 2 and the Agilent can be seen in Figure 3.3. The boxes encompass a given percentage of each type of point. For both data sets, it is clear that the predicted internal standard generally offered the lowest error. Rh offers very low error as well, especially in the Agilent.

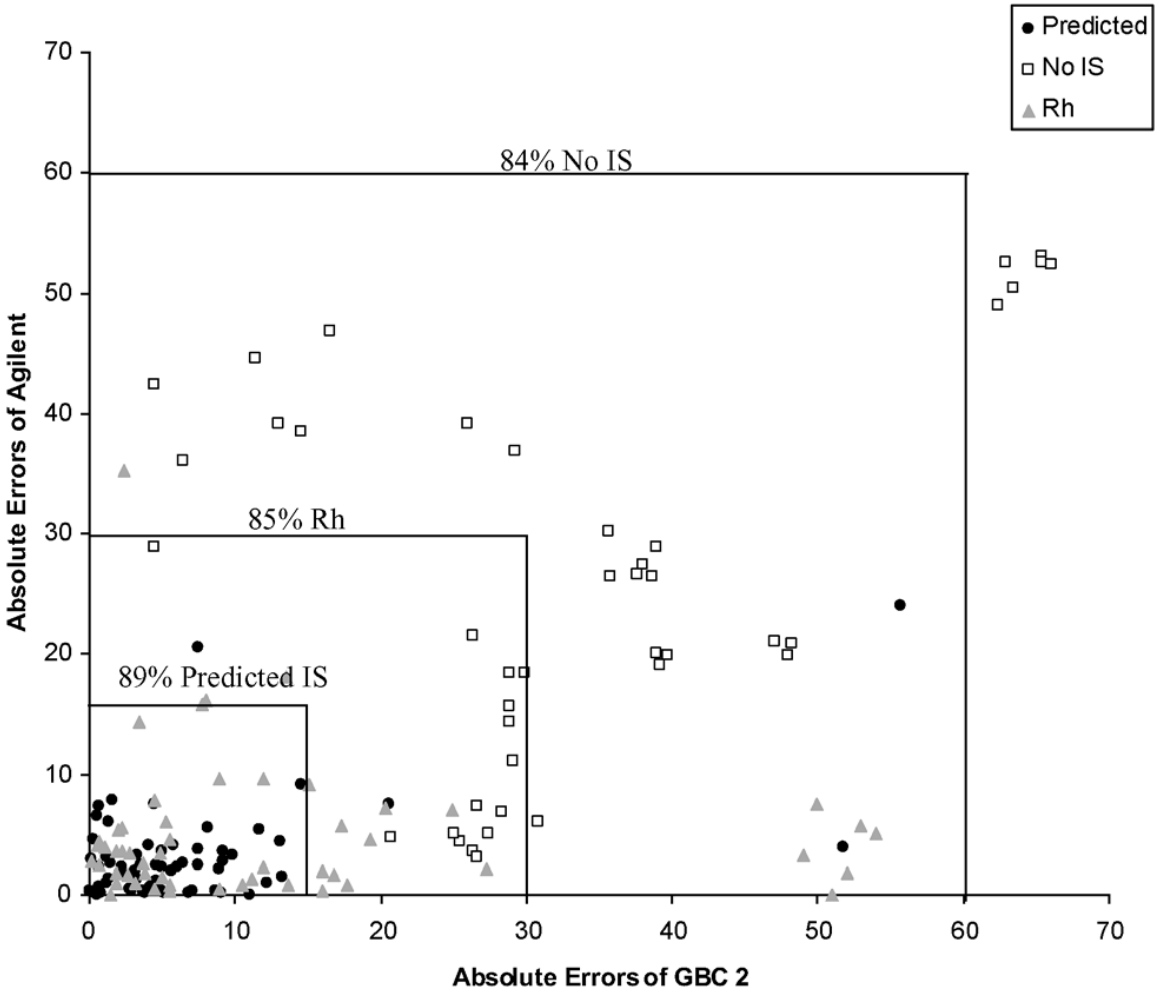

Figure 3.3. Scatter plot comparing errors of the predicted IS, no IS and using Rh as an IS for all analytes. The errors of GBC 2 are plotted against those of Agilent. The data points represent resulting errors when using predicted internal standards (●);using no internal standard (□); and using Rh as the internal standard (▲).

3.3.3 Evaluation of General Trends When Comparing All Three Data Sets

The majority of data indicate that it is better to use *any* internal standard than it is to calibrate with no internal standard. Exceptions to this existed primarily among the light elements such as Be and Mg. These elements exhibit signal trends that differ

greatly from the majority of other elements in solution; and hence, few internal standards were useful in compensating for the signal variations.

Naturally, if the analyte signal does not change as a result of the given system perturbation, the error will be very low. For example, the 6 mm torch position in GBC 2 did not significantly perturb the system which led to very low errors for "No IS." Therefore, the uncertainty added when taking the ratio resulted in larger errors from internal standardization. Figure 3.4 summarizes the number of elements at each perturbation where one or more elements used as internal standards gave a higher error than using no internal standard.

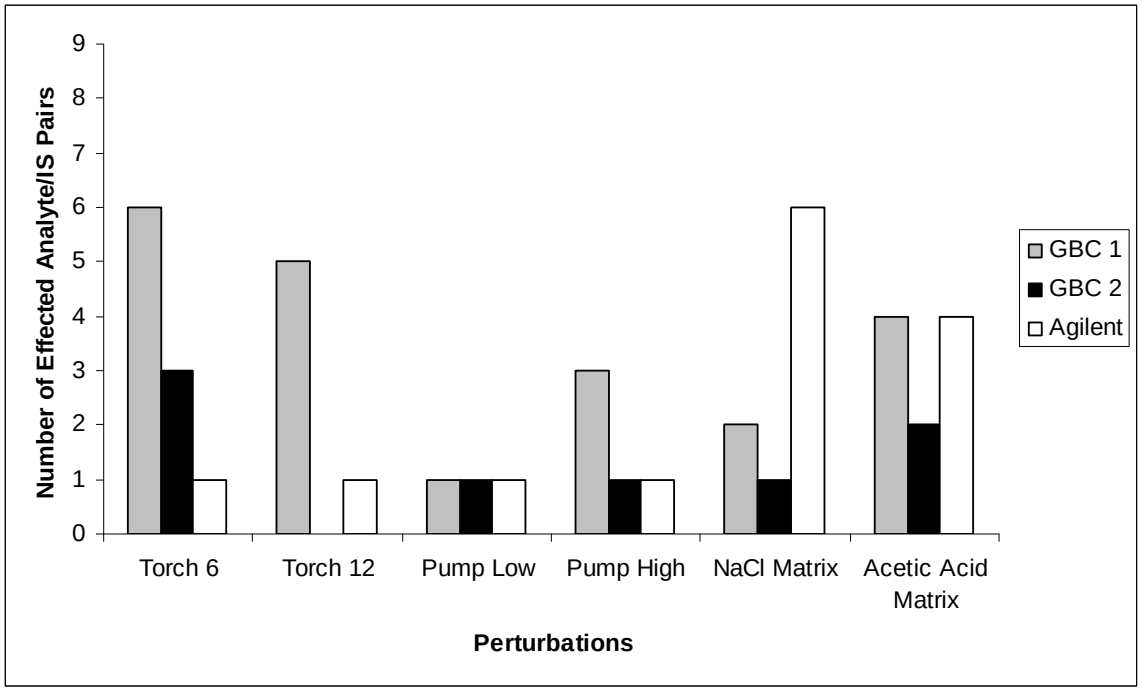

Figure 3.4. Number of analyte/IS pairs that exhibited higher error in concentration than analyses run using no internal standard.

A number of studies agree that internal standard choice should be governed by similarities in mass with the analyte of interest[1,2] even though it was also shown that such criteria is not infallible.[10] Figure 3.5 represents the number of analyte/IS pairs that were closest in mass *and* exhibited the lowest error in concentration.

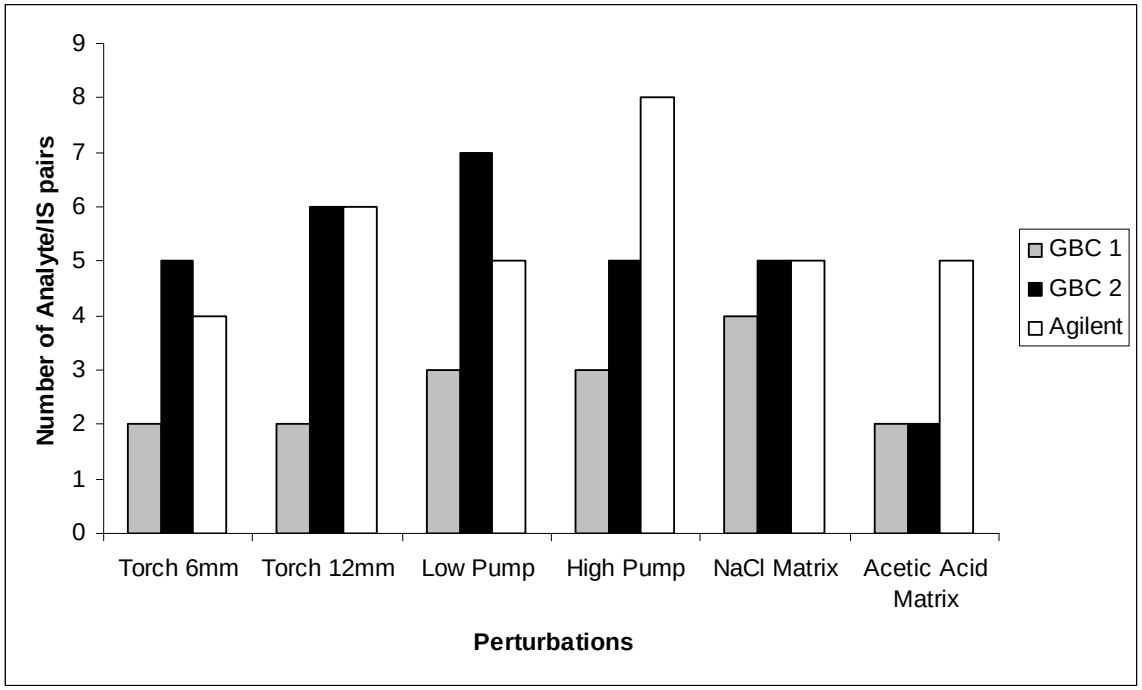

Figure 3.5. Number of analyte/IS pairs which were the closest in mass and whose errors were better or equal to the lowest error observed. (Statistical uncertainty was taken into account in making this decision.)

It is clear from perturbations such as the acetic acid matrix that an IS choice based only on mass similarity would lead to a less-than-optimal internal standard choice. Just over half followed a mass trend in the Agilent and only two of nine pairs from GBC 1 and 2. It is clear that GBC 1 has the weakest overall mass dependency. In GBC 2 and the Agilent there are many cases for a given perturbation and a given analyte where the errors are not statistically different, regardless of the internal standard used. Therefore,

some of the pairs included in Fig. 6 reflect these small errors and may not necessarily support the presence of a mass dependency on IS selection.

From Figure 3.5 it is difficult to isolate particular perturbations that offer a stronger or weaker mass dependency for all instruments. This plot suggests, however, that the pump rate perturbations offer a relatively strong mass relationship. This follows the multiple ordinary least squares regression trends found previously.[10] The acetic acid matrix had a relatively low mass dependence for all three data sets, which also followed the previously established OLS trends.

Another parameter thought to impact internal standard behavior is ionization potential.[1] Figure 3.6 represents the number of analyte/IS pairs that were closest in ionization potential *and* exhibited the lowest analysis errors.

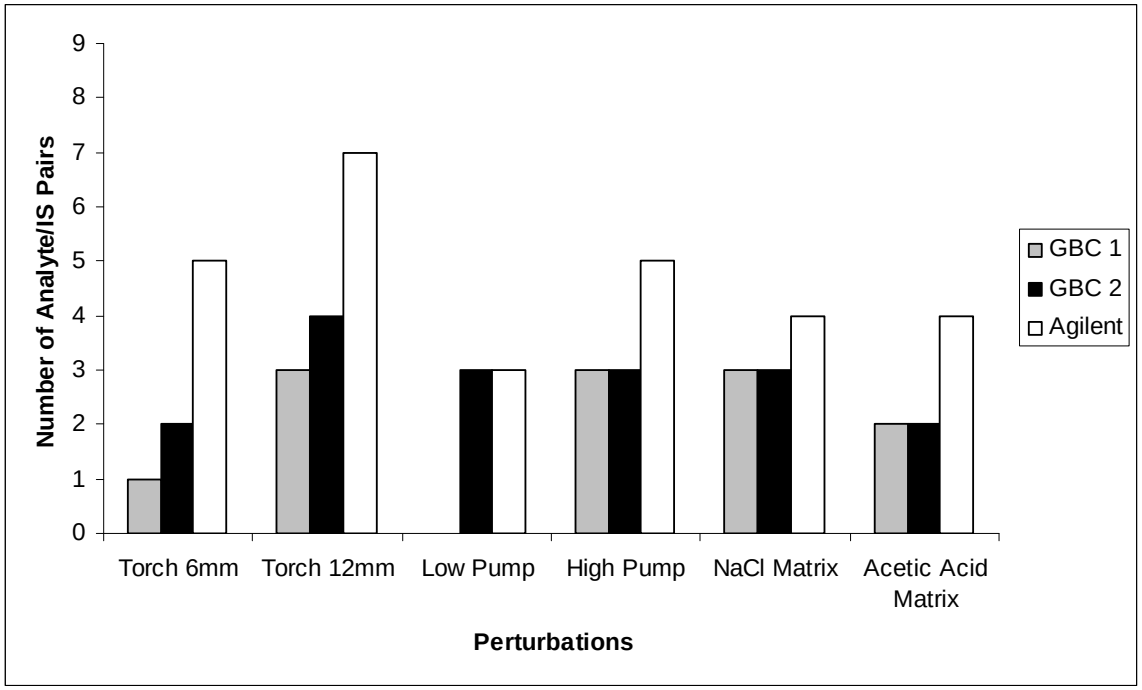

Figure 3.6. Number of analyte/IS pairs that exhibited the lowest error and were closest in first ionization potential.

Clearly, there is less dependency on ionization potential than there is on mass, which is expected from previous results.[10] Although the Agilent data indicates a stronger relationship to ionization potential, it is most likely an artifact of the errors not being statistically different from one another, as previously discussed. The perturbation that seemed to be most affected by ionization potential was the movement of the torch farther from the sampling cone, viz., "12 mm torch position." This may be a result of a drop in temperature as sampling is conducted farther from the optimum distance relative to the load coil. Therefore, ionization efficiency of the element may become a more significant factor. However, there are no apparent trends among the ionization potentials of the anlalyte/IS pairs exhibiting this relationship.

3.4 CONCLUSIONS

The current study suggests that the performance of the prediction scheme presented previously[10] remains remarkably reliable not only for the same instrument (viz., GBC ICP(TOF)MS) months later but also for a totally different ICPMS platform (viz., Agilent quadrupole ICPMS). The data also complemented the mass and ionization potential relationships determined earlier[10], insofar as similarities in mass were of greater importance to analyte/IS performance. However, it is still clear that choosing an internal standard based on similarities in mass alone could be problematic. Similarly poor results frequently appeared when attempting to use the same internal standard (*e.g.*, Rh) for all analytes.

Internal standard choice was apparently less crucial in GBC 2 and the Agilent, which often offered excellent accuracy regardless of IS choice. However, this was highly dependent on the analyte of interest and the particular perturbation being considered. Thus, while selection of a good internal standard currently has no predictive equation, it appears from the studies thus far that a good analyte/IS pair that is selected from the

prediction set[10] may have reasonable applicability over time and instrument platform variations.

3.5 ACKNOWLEDGEMENTS

This work was supported in part by the Robert A. Welch Foundation. The authors would also like to thank Nathan Miller for his assistance in gathering data on the ICP(quadrupole)MS.

3.6 REFERENCES

1. J. J. Thompson and R. S. Houk, *Applied Spectroscopy*, 1987, **41**, 801-806.

2. F. Vanhaecke, H. Vanhoe, R. Dams and C. Vandecasteele, *Talanta*, 1992, **39**, 737-742.

3. C. Sartoros and E. D. Salin, *Spectrochimica Acta, Part B: Atomic Spectroscopy*, 1999, **54B**, 1557-1571.

4. C. Vandecasteele, M. Nagels, H. Vanhoe and R. Dams, *Analytica Chimica Acta*, 1988, **211**, 91-98.

5. J. Wang, W. L. Shen, B. S. Sheppard, E. H. Evans, J. A. Caruso and F. L. Fricke, *Journal of Analytical Atomic Spectrometry*, 1990, **5**, 445-449.

6. J. Wang, E. H. Evans and J. A. Caruso, *Journal of Analytical Atomic Spectrometry*, 1991, **6**, 605-608.

7. M. Y. Perez-Jordan, J. Soldevila, A. Salvador, A. Pastor and M. de la Guardia, *Journal of Analytical Atomic Spectrometry*, 1999, **14**, 33-39.

8. J. Dombovari, J. S. Becker, A. J. Kuhn and W. H. Schroder, 2000, 79-89.

9. M. Wang, *Yejin Fenxi*, 2004, **24**, 19-22.

10. H. J. Finley-Jones, J. L. Molloy and J. A. Holcombe, *Journal of Analytical Atomic Spectrometry*, 2008, **23**, 1214-1222.

Chapter 4: Determination of Metal Association for Labile Metalloprotein Complexes Using BN-PAGE with a Modified Electroblot and ICPMS

4.1 INTRODUCTION

Although it has been estimated that 30% of proteins are associated with a metal, there currently exists no rapid means of determining the specific protein-metal associations in a large and complex protein mixture such as that present within a cell. It has been speculated that polyacrylamide gel electrophoresis (PAGE) might be the most viable separation technique to ultimately accomplish this goal.[1-4] Multi-dimensional PAGE offers the highest resolution and sample capacity of all the protein separation techniques.[5] In addition to its potential separation capabilities, the gel surface and the raster scanning capabilities of laser ablation inductively coupled plasma mass spectrometry (LA-ICPMS) appear to be well-matched. As a result, the coupling of PAGE and LA-ICPMS has grown in popularity over the last several years as one approach to characterize metalloproteins.

Neilsen et al.[6] were the first to suggest that metalloproteins could be detected on a polyacrylamide gel using laser ablation sampling and ICPMS detection. In 1999, Lustig et al. [7] explored the use of 1-dimensional isoelectric focusing to determine the presence of metalloproteins in both human and rabbit serum that had been incubated in a variety of isotopically enriched metal standards. Since then, a number of studies have explored various operating conditions and procedures with PAGE for their efficacy in characterizing metalloproteins. The use of a charge shift molecule is one such condition.

Sodium dodecyl sulfate (SDS) is routinely used in such a role for both 1-D and 2-D separations (SDS-PAGE). This separation approach was used in several studies where metal-protein associations were sought.[5,8-21] Unfortunately, the excellent *protein* separation provided by SDS-PAGE, frequently destroys any metal-protein associations of the native protein because of extreme denaturation by SDS.[15, 19, 21]

Another charge shift molecule that has been considered for this application is Coomassie Brilliant Blue, utilized in blue native (BN) PAGE. Unlike SDS, Coomassie is considered to be non-denaturing, and has therefore been found to be more effective for non-covalently bound metals.[21-24] Clear native (CN) PAGE offers the most limited disturbance to the protein's native state and subsequent metal binding characteristics. CN-PAGE has also been explored for metallomics applications[19-21] despite its significant decrease in resolution compared with the other techniques described.[25] Examples of other operating conditions that have been studied include metal sequestration by protein stains[24] and even competitive metal binding from the electrophoretic running buffers.[21]

Once the protein separation is complete, the gel is often dried and ablated directly. However, a couple of studies have utilized the technique of electroblotting the protein from the gel to another surface, thereby enhancing S/N.[11, 20]

The present study seeks to expand on this groundwork, utilizing BN-PAGE and a uniquely modified electroblot system for enhanced capture followed by analysis with LA-ICPMS. It is clear that three criteria must be met if a systematic multielemental determination of metal-protein associations is to be obtained: 1) a protein separation with minimal or no denaturation; 2) a separation environment where equilibrium promotes metal *association with* and not *dissociation from* the host protein; 3) a sufficiently low

metal background after separation so that optimal sensitivity and a maximum dynamic range can be realized. The first criterion is met through the use of either BN- or CN-PAGE. Fulfillment of the second criterion is dependent on the equilibrium relationships between the proteins and metals within a specific system. At one extreme are the very weakly associated alkali metals and some alkaline earths. At the other extreme are those whose binding is sufficiently strong that the protein is unlikely to lose the coordinated metal unless significant denaturation occurs. Most metalloproteins are likely to fall somewhere between these two extremes. Using separation buffers with elevated metal concentrations may work to push equilibrium toward complexation or maintain the *in situ* metal-protein association during the separation procedure.

However, the metals added to the separation buffer can reduce S/N if the gel is ablated directly. Elevated free metal in the separation buffer can also result in the coordination of the metals to weak sites on a protein even though the metal would not normally be considered part of the metalloprotein under normal cellular conditions. Orthogonal transfer of proteins across the gel thickness to a blotting membrane (electroblotting) using a metal-free transfer buffer offers a potential solution to the previous concerns. In traditional electroblotting the negatively charged proteins migrate toward the anode in the presence of an electric field. A blotting membrane is used to capture the migrating proteins and concentrate them on the surface for further analysis. Common blotting membranes include polyvinylidene fluoride (PVDF), nitrocellulose and less frequently, quartz fiber filters.

The present study utilizes electroblotting to monitor both migrating protein *and* free metal cations that move in the opposite direction toward the cathode during the

blotting procedure after the BN-PAGE separation. Although blotting membranes are effective for capturing proteins, they are not necessarily designed to have good affinity for free metal cations. Chemical modification of the blotting membrane surface, however, may improve both protein and free metal capture. Unlike PVDF, silica surfaces are relatively easy to modify for subsequent covalent attachement of other molecules.[26-29] Three chemical modifications of the silica surface compared are: an acid hydrolyzed surface, a silanized surface using (3-mercaptopropyl) trimethoxysilane (3-MPS) and a surface onto which poly acrylic acid (PAA) has been covalently attached. These surfaces will be evaluated for both protein *and* metal capture capabilities. Silanization with 3-MPS yields surface thiols, which have demonstrated good affinity for soft acid as well as large biomolcules.[30] PAA yields surface carboxylate groups, which should offer improved affinity for harder acid metals such as Cu^{2+}.

As many previous studies have suggested, it is important to demonstrate proof-of-concept with well-characterized metalloproteins.[21,23,24] Unfortunately there are no reference materials for which the metals complexed nor their formation constants are unequivocally known. However, bovine serum albumin (BSA) has been the focus of numerous studies and should serve as a "model compound". BSA is a blood plasma protein that contains two relatively strong Cu binding sites in addition to a free cysteine.[31,32] Because it is well characterized and relatively stable in solution, BSA is a reasonable test protein for the preliminary development of any approach whose end goal is the development of a rapid screening tool. Although BSA is well characterized and is typically considered a "strong" copper binder, a large range of binding constants (ca. 10^4-10^{14}) have been reported and were summarized by Masuoka et al.[33]

In order to locate the protein using ICPMS despite potential Cu loss, Ag will be used to tag the free cysteine present on BSA. Ag^{2+} binds very strongly to cysteine ($K_f = 10^{13}$)[34] and is unlikely to equilibrate into solution. This, coupled with a very low background at m/z=107 and excellent sensitivity make it a good measure of relative protein amount.

4.2 EXPERIMENTAL

4.2.1 Instrumentation

Separations were conducted using the NativePAGE™ Novex® Bis-Tris Gel System and electroblotting was done with an XCell II™ Blot Module (Invitrogen). Both utilized a PowerEase® Programmable Power Supply (Invitrogen). All separations were run for 1.5 h at 150 V. All electroblotting was conducted at 4 V, except where noted.

Samples were ablated with a Quanta-Ray® DCR-11 Pulsed Nd:YAG laser (Spectra-Physics) operated at 1064 nm. Operating parameters are listed in Table 4.1.

Table 4.1. Laser ablation operating parameters.

Wavelength (nm)	1064
Pulse Width (ns)	8-9
Pulse Energy (mJ)	275
Pulse Repetition Rate (Hz)	10 (optimal)
Ablation Spot Size (μm)	100 (approximate)
Scan Rate (mm/s)	0.25-1.0

Time resolved, single shot ablation studies indicate a signal 1/e decay time of 4 s. The laser was scanned across the BSA bands on the electroblot strips and dried gel. The scan rates were varied to determine optimal S/N vs. resolution. Data were collected on a GBC

Optimass 8000 (GBC Scientific, Hampshire, IL, USA) ICP orthogonal time-of-flight mass spectrometer. ICPMS parameters are listed in Table 4.2.

Table 4.2. ICP(TOF)MS optimized parameters for maximum dry plasma sensitivity.

Acquisition Time (s)	Variable, based on ablation distance
Number of Replicates	3 scans
Optimized Torch Position X, Y, Z (mm)	10, -0.5, 0.1
Sample Gas Flow (L/min)	1.01
Plasma Gas Flow (L/min)	10.000
Auxiliary Gas Flow (L/min)	1.300
Generator Set Power (W)	700

To ensure that the results were not skewed because of the choice of laser and/or mass analyzer, a second LA-ICPMS system was also employed. This system consisted of a NewWave UP193-FX eximer laser emitting at 193 nm coupled to an Agilent 7500cx (Agilent Technologies, Foster City, CA) ICP quadrupole mass spectrometer.

4.2.2 Reagents

Bovine serum albumin (Fisher) was purchased as a 20 mg/mL purified solution. HPLC analysis of the BSA solution was conducted using a Gold Gradient HPLC (Beckman Systems) fitted with a C18 0.80×250 mm column (Selfpak). This analysis indicated BSA purity of 95%. SDS-PAGE confirmed the presence of non-BSA species which have not been further characterized. Cu^{2+} (SPC Science) and Ag^{2+} (Inorganic Ventures) metal standards were used during protein preparation and separations.

NativePAGE™ 4-16% Bis-Tris Gels (Invitrogen) were used for all separations. Cathode, anode and transfer buffers (Invitrogen) were prepared according to the manufacturers' instructions. The cathode buffer is identical to the anode buffer except that it contains Coomassie. The transfer buffer was analyzed for metal content and was found to contain no Cu or Ag above the blank (0.1 ppb for Cu, 0.02 ppb for Ag). (3-mercaptopropyl) trimethoxysilane (Acros Organics), poly-acrylic acid (Acros Organics) and methanol (Fisher) were used for the electroblot membrane functionalization.

4.2.3 Procedures

4.2.3.1 Blue Native Polyacrylamide Gel Electrophoresis and Electroblotting

Each gel lane was loaded with 20 μL of prepared protein solution. Both the cathodic and anodic running buffers were loaded with 200 ppb (3 μM) Cu^{2+}. More than one band was observed using BN-PAGE, which can be attributed to the impurities discussed previously and possibly BSA aggregation due to high protein concentration. Gels that were not to be electroblotted were dried at 80 ºC for 1 h on a Model 583 Bio-Rad gel dryer.

For electroblotting, the gel casing was removed and 6 × 80 mm membrane strips (acid hydrolyzed quartz fiber, silanized quartz fiber or PVDF) were applied over each lane on both sides of the gel. Upon removal, the strips were dried in an environmental hood prior to analysis.

4.2.3.2 Electroblot Membrane Modification

Quartz fiber filters (QM-A Whatman) were cut into 6 × 80 mm strips in accordance with the width of a lane and the length of the gel being used. The strips were *acid hydrolyzed* by boiling in trace metal grade 25% v/v HNO_3 (Fisher) for 30 min. Some acid activated strips were then *silanized* with (3-mercaptopropyl) trimethoxysilane (3-MPS) after the procedure of Miller et al. for silanization of controlled pore glass.[27] Briefly, 3-MPS was dissolved in MeOH under N_2 for approximately 5 min. The quartz fiber sheets were added to the reaction vessel and refluxed under N_2 at 60 ˚C for 6 h. The filters were subsequently rinsed with MeOH and air dried in a 100 ˚C oven for 12 h. Some of the silanized strips were subsequently modified with poly acrylic acid (PAA) using a procedure described in full by Miller et al. [27]

4.3 RESULTS AND DISCUSSION

4.3.1 BN-PAGE of BSA

Figure 4.1a is a photograph of a gel lane containing the separated BSA solution. This specific gel has been stained with Coomassie Brilliant Blue ™ after separation to enhance contrast for this figure only. None of the gels used for ICPMS analysis was stained after the separation. The line represents the ablation path of the laser, and the arrow illustrates the direction of ablation. From this image, it is clear that there are other bands present besides that of monomeric BSA. The presence of uncharacterized impurities is further illustrated in the 1-D SDS-PAGE separation shown in Figure 4.1b. All data shown utilizes BSA concentrations of 1-10 mg/mL. As a point of reference, serum albumin is present in blood at concentrations of 35-55 mg/mL.[35]

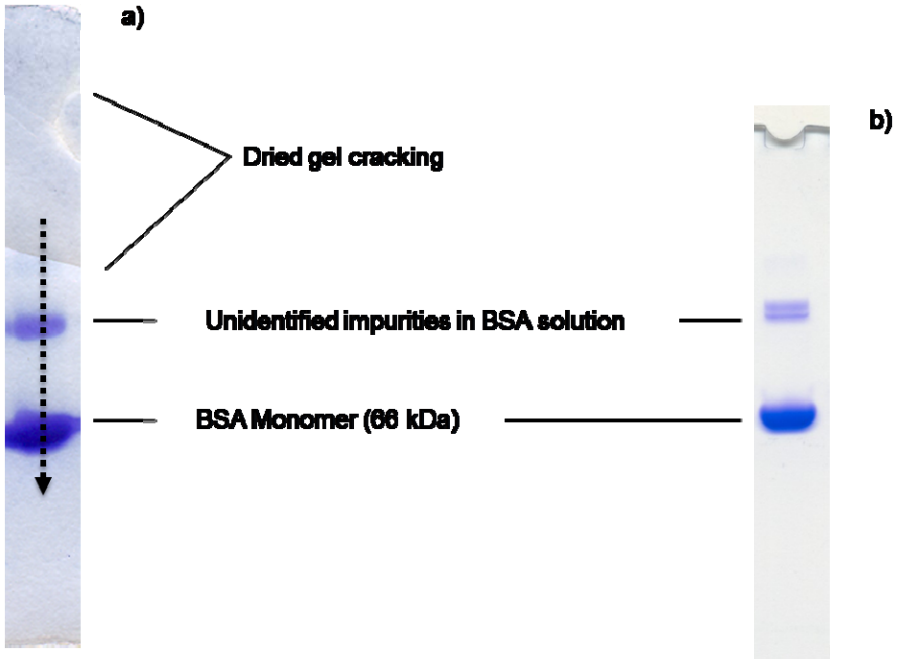

Figure 4.1. a) BN-PAGE gel lane that has been stained for visual clarity. This specific gel was not used for analysis. The line represents the approximate location and length of the ablation in the direction indicated by the arrow. b) 1-dimensional SDS-PAGE of BSA solution.

It is important that the relevant protein-metal complexes remain intact until the time of analysis. Metal loss from a labile complex is highly dependent on the local environment and will occur in the presence of a metal-free buffer. The rate of loss is a function of the OFF rate as well as the thermodynamic stability of the complex. Analysis of the PAGE running buffer indicated a copper concentration of approximately 2 ppb (30 nM). If this were the equilibrium Cu^{2+} concentration in the gel where the protein was positioned, then ~ 50% of the Cu binding sites would be occupied for a metal-protein complex whose K_f ~$3x10^7$. To promote equilibrium retention of metals, Cu^{2+} was increased to 200 ppb (3 μM) in the running buffer. In effect, this would allow exploration of even more weakly complexed metals (viz., K_f ~ $3x10^5$), assuming equilibrium

attainment. The concentration of various free metals within a cell are estimated to range from ~10^{-13} M for Cu to 10^{-2} M for Mg. These values are based on estimates of formation constants between the specific metals and surrounding proteins.[36] The very large amounts of dry mass within a cell[37] may lead to metal activity coefficients of 10-100,[38] thus increasing the effective free metal concentration by 1-2 orders of magnitude.

In the case of BSA, LA-ICPMS results indicate an average of about four times more Cu in the protein band when the separation running buffers are loaded with 200 ppb Cu in place of the 2 ppb Cu impurity level. This was determined after 10 min of electroblotting, which allows ample time for the extraction to the cathode of free Cu^{2+} in the gel as well as Cu^{2+} weakly adsorbed to the protein. This data can be used to estimate an approximate K_f for the BSA-copper complex if we assume equilibrium conditions persisting at all spatial locations during the blotting process. Considering only a single Cu binding site, at equilibrium we can assume:

$$K_f = \frac{[ML]}{[M][L]} \tag{4.1}$$

where [ML] represents the copper-BSA complex while [M] and [L] represent uncomplexed Cu^{2+} and BSA active site concentrations, respectively. Using the information obtained under both free Cu^{2+} concentrations, we can derive the following relationship:

$$K_f = \frac{[ML]_{2\ ppb}}{[M]_{2\ ppb}[L]_{2\ ppb}} = \frac{[ML]_{200\ ppb}}{[M]_{200\ ppb}[L]_{200\ ppb}} \tag{4.2}$$

Using the mass balance for binding sites

$$[L]_T = [L] + [ML] \tag{4.3}$$

and the experimentally determined relationship of $[ML]_{200\ ppb} = 4[ML]_{2\ ppb}$; a solution for $[ML]_{2\ ppb}$ and $[ML]_{200\ ppb}$ can be determined. $Log\ K_f$ can then be estimated at 6. The precision for $[ML]$ is poor but probably impacts the estimated $log\ K_f$ by less than ± 1. Interestingly, this K_f indicates that the 2 ppb copper impurity in the separation buffer should result in only about 5% of the BSA being loaded with copper.

In general, metal loading of the buffers will increase in importance as weaker protein-metal interactions become of interest. It should be noted that BSA is also assumed to bind Zn^{2+} in a biological system and has shown affinity for several other metals.[32] However, this study will confine itself to consideration of the copper-BSA complexation.

As expected, the Cu loading of separation buffers resulted in a noisy Cu background when the gel was ablated and the ICPMS signal analyzed. This made it difficult to make confident *qualitative* statements regarding the presence of Cu above background noise levels in the region where the BSA was located and confirmed the postulate that free and weakly bound copper must be removed to achieve a reasonable S/N.

Electroblotting with the use of a metal-free transfer buffer effectively accomplished this. Based on the electrophoretic mobility of Cu^{2+} and an electroblot potential of 4 V, it is estimated that all free Cu^{2+} will migrate through the thickness of the gel and to the cathode membrane in approximately 2 min. This calculation assumes that the gel pore diameters are much greater than the hydrated Cu^{2+}. Blotting membrane strips were placed both on the anode and the cathode sides of the gel. Ideally, the

"anodic membrane" will capture the Coomassie-loaded BSA while the "cathodic membrane" would collect any free Cu^{2+} that dissociated from the protein.

4.3.2 Comparison of Different Blotting/Ablation Substrates

Four different substrates were evaluated for relative sensitivity and capture efficiency during the electroblot. The four substrates included PVDF, acid hydrolyzed quartz fiber and silanized quartz fiber as well as the dried gel. The separation was run using 20 μL of 1 mg/mL BSA per lane. Upon completion of the separations, PVDF, acid hydrolyzed and silanized blotting strips were placed on both the anodic and cathodic sides of the gel. One lane was cut from the gel and dried for later analysis.

The blot was run at 4 V and blotting strips of each substrate type were removed at 2, 10 and 30 min. It should be noted that this is a significantly lower voltage and shorter time than the manufacturer's suggestion of 30 V for 1 h. The lower voltage was utilized to decrease free metal ion velocity in order to gain meaningful, time-resolved information at the cathodic membrane.

Both the blot on the anodic (protein) side as well as the dried gel were sampled by laser ablation and analyzed with the ICP(TOF)MS. The Ag signals of each blotting substrate were compared to determine which offered the highest sensitivity and/or protein retention efficiency. Reproducibility studies indicate an average strip-to- strip uncertainty of 60%.

Figure 4.2 illustrates the results after a 30 min electroblot onto acid hydrolyzed quartz, silanized quartz and PVDF. The LA-ICPMS signal from a dried gel before electroblotting is also shown. The $^{107}Ag^{+}$ signal on the protein side comes from the Ag-

cysteine tagging of the BSA and serves to identify the BSA as well as to provide a measure of relative protein amount. The graphic insert in this figure uses an expanded scale to show differences in the weaker signals. It is clear that the protein capture and/or ablation efficiencies are significantly better using the silanized quartz blotting membrane.

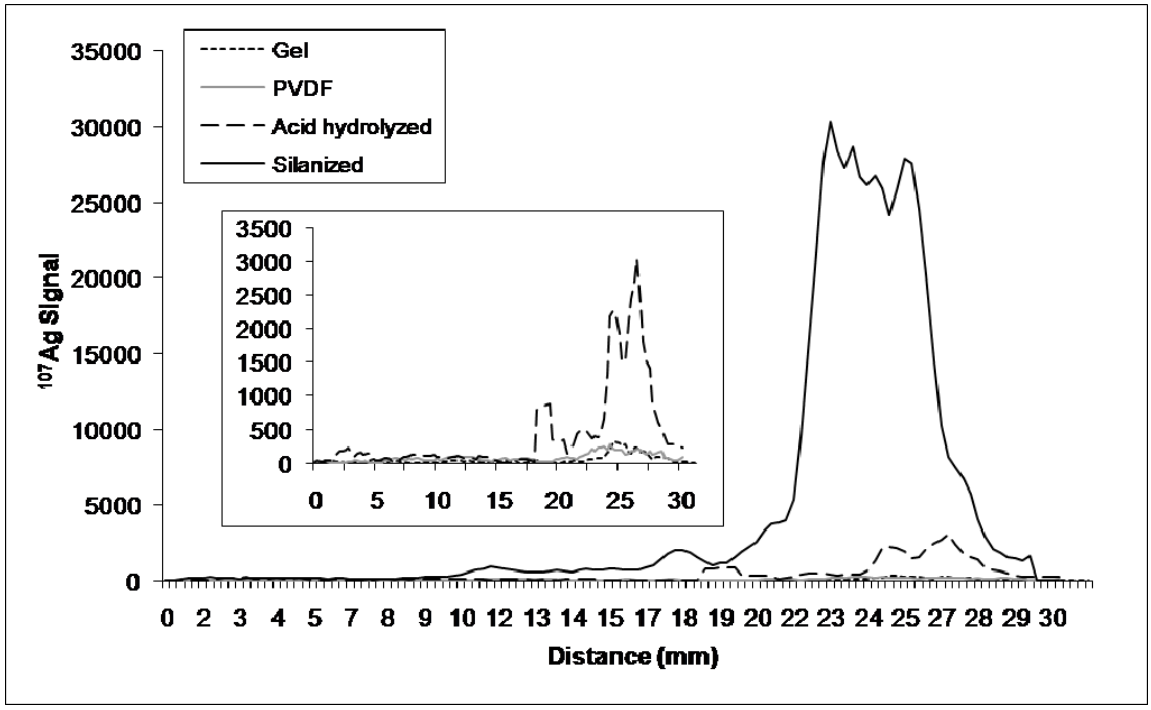

Figure 4.2. Comparison of different substrates for electroblot transfer efficiency and/or sensitivity. The inserted plot depicts a 10X magnification in order to observe substrates other than silanized quartz.

The Comassie-stained BSA band on the silanized membrane strips is also visually darker than the acid hydrolyzed and PVDF strips following the electroblot, thus supporting the suggestion of improved protein capture efficiency. Since the unblotted dried gel *should* contain the most BSA and Cu of all the considered substrates, it is suspected that the lack of sensitivity results in part from poor ablation characteristics.

When using the 1064 nm laser, extensive cracking and a large variation in ablation spot size was observed. It is widely accepted in the literature that a lower wavelength laser produces more uniform ablation spots. Therefore, it was decided to compare the silanized electroblot membrane to the dried gel using a 193 nm eximer laser with a different ICPMS system in order to confirm that the trend from Figure 4.2 was not laser or instrument specific. The results are shown in Figure 4.3 for ablation of a dried gel and of a silanized membrane that was electroblotted for 10 min at 4 V. The 193 nm laser significantly improved the ablation spot shape and uniformity with the dried gel. The sensitivity using the dried gels also improved, but the ablation of a silanized electroblot membrane continued to produce a larger $^{107}Ag^{+}$ signal while scanning over the BSA band. This may be explained by the effective preconcentration of protein on the surface of the thin silica elctroblot membrane while the protein was distributed throughout the thickness of the dried gel. Additionally, dried gels have a tendency to curl and are prone to cracking, thus making them significantly more difficult to keep within the focal plane of the ablation optics.

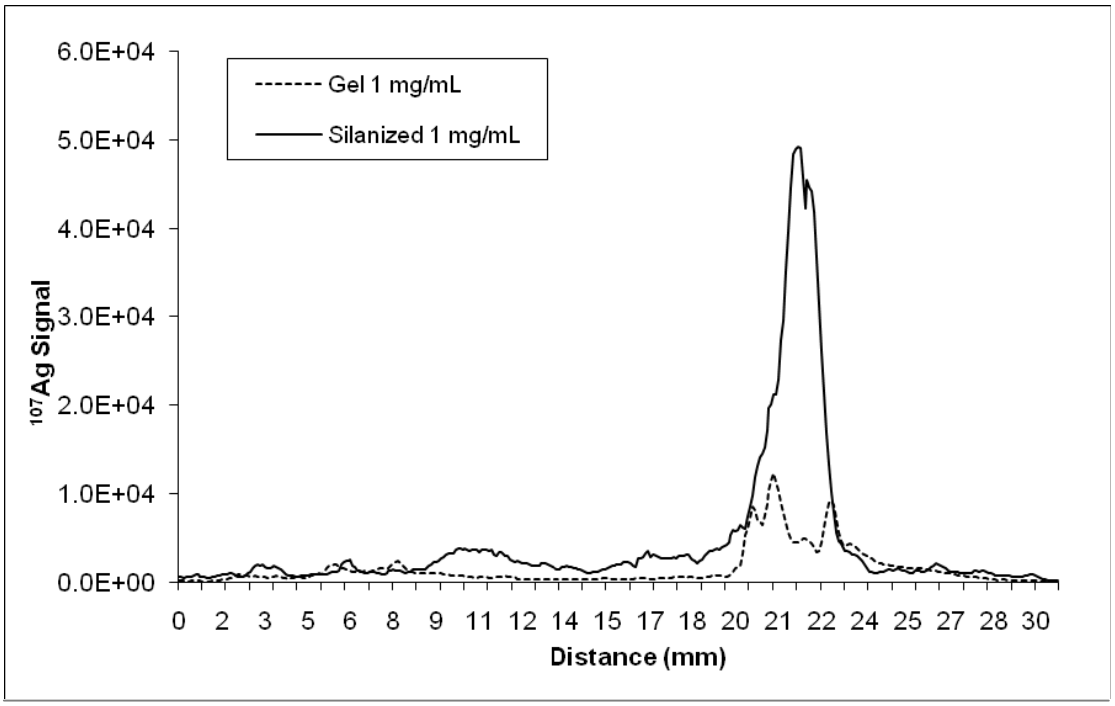

Figure 4.3. Analysis of BSA ablation of dried gel and silanized quartz fiber membrane with 193 nm eximer laser.

4.3.3 Equilibration of Non-Covalently Bound Metals

The $^{107}Ag^{+}$ signal taken at different blotting times in Figure 4.4, shows that the protein is accumulating at the anode membrane (silanized surface) over the course of the experiment.

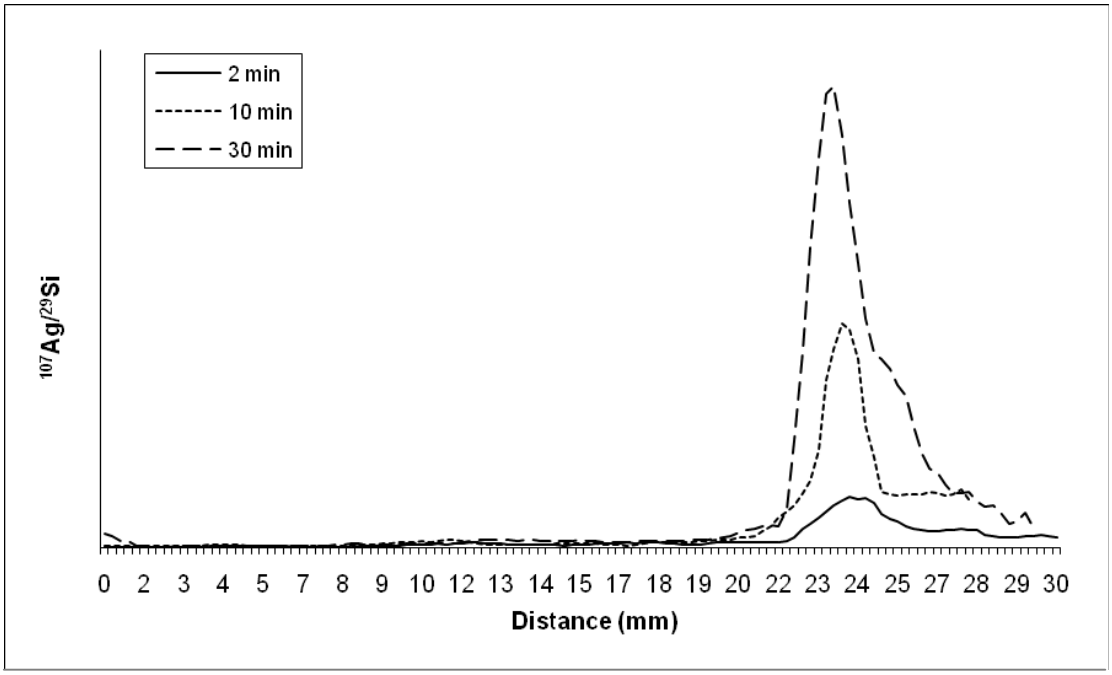

Figure 4.4. Protein accumulation over time as represented by accumulation of Ag at the silanized anode membrane of the electroblot.

Conversely, Figure 4.5 illustrates a different trend with respect to the $^{63}Cu^{+}$ signal. It is logical that 10 min of electroblotting should offer a larger $^{63}Cu^{+}$ signal than 2 min since very little protein will have migrated after only 2 min at 4 V. Despite the increase in protein, it is also clear that the protein-bound Cu is almost completely lost between data collected at 10 min and 30 min. This decrease in signal over time likely results from the equilibrium driven, time-dependent dissociation of the metalloprotein and the inability of blot membrane's silanized surface to strongly complex and retain the Cu^{2+}. The cause of the elevated $^{63}Cu^{+}$ background in Figure 4.5 is not clear, but it is not due to transport of free Cu^{2+} in the gel to the silanized silica membrane since the data shown is from the anodic side of the gel.

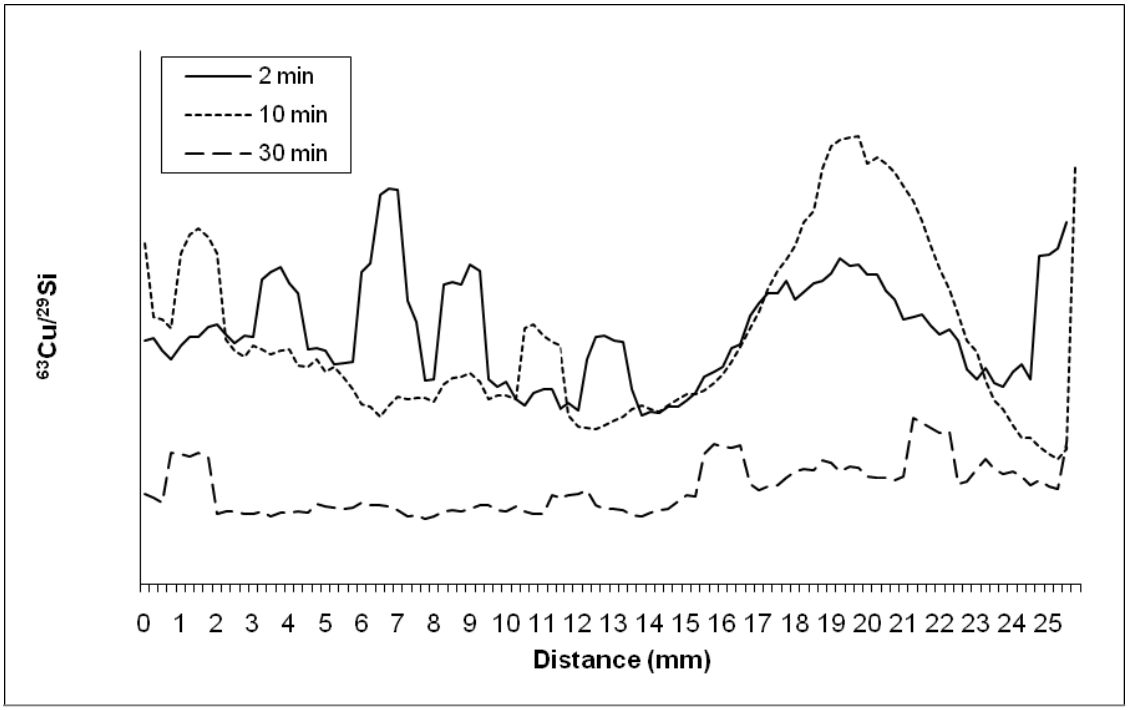

Figure 4.5. Cu signal monitored on the anode transfer membrane during 4 V electroblot process over time. Ablation from silanized quartz fiber membrane. 10 mg/mL BSA was loaded into each lane.

From Figure 4.5, it is clear the Cu^{2+} is equilibrating away from BSA as blotting proceeds in metal-free transfer buffer. It is expected that the Cu^{2+} released from the protein should either complex with the anodic membrane's thiols or begin back through the gel toward the cathode. At the cathodic membrane, Cu^{2+} will either complex with the silanized membrane or move through the membrane into the buffer solution. Since the anodic membrane's $^{63}Cu^{+}$ signal decreases after 10 min, it is unlikely that the silanized surface is efficiently binding the free Cu^{2+}.

Figure 4.6 shows the results from analyzing the membrane placed on the cathodic (-) side of the gel. At 2 min, there are two distinct ^{63}Cu peaks at approximately 13 and 23 mm. The peak at 23 mm is attributed to Cu lost from BSA based on its location relative to the Ag-tag peak. As discussed previously, it should take a maximum of approximately

2 min for free Cu^{2+} to move through the gel and onto the cathodic blotting membrane. Therefore, these two peaks may result from the free ions dispersed throughout the gel as well as the Cu^{2+} very weakly adsorbed to, for example, the BSA surface. Although the Cu that is lost from the BSA is present on the cathode membrane at all three times, there is an apparent decrease in signal after 2 min rather than the expected increase. This again illustrates an inefficient Cu^{2+} retention by the silanized quartz surface.

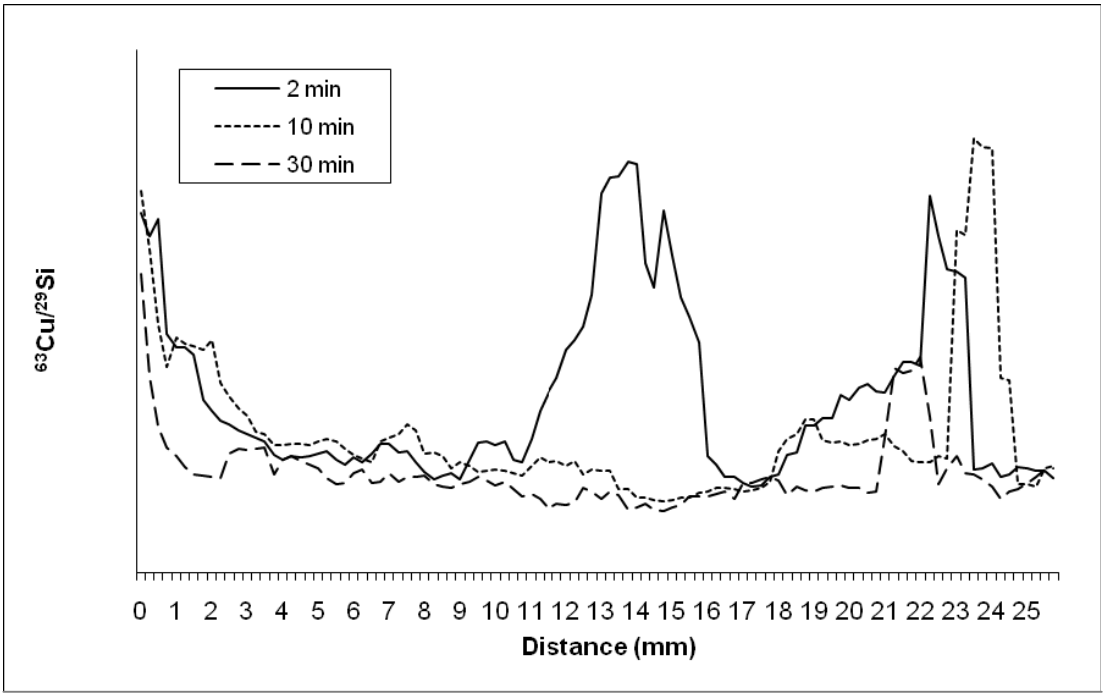

Figure 4.6. Cu signal monitored during 4 V electroblot process on the cathode side of the electroblot. Ablation from silanized quartz fiber membrane.

The accumulation of protein on the anode membrane with time is attested to by the increasing $^{107}Ag^{+}$ signal from the Ag-cys tag on the BSA. The decreasing Cu^{2+} signal on the anodic membrane suggests that a) a significant amount of Cu^{2+} is dissociating from the BSA , and b) the Cu^{2+} is not being retained by the silanized membrane once released. The Cu^{2+} membrane binding results are not totally unexpected since thiols

typically coordinate strongly with soft acid metals but not particularly strongly with hard acid metals such as Cu^{2+}.

4.3.4 Blotting Membrane Modification for Enhanced Cu^{2+} Capture

Poly-acrylic acid (PAA) was immobilized onto the quartz blotting membranes to explore the possibility of enhancing the Cu^{2+} capture efficiency. BN-PAGE was run with 1 mg/mL BSA loaded into all wells and Cu loaded buffers. Electroblotting conditions were the same as those previously described. Quartz fiber membranes that were modified with PAA were placed over each lane at both the anodic and cathodic sides of the gel as was done previously with the other modified blot membranes. Based on the $^{107}Ag^{+}$ signal at the anode, both the silanized and PAA-modified surfaces improved protein capture when compared with the acid hydrolyzed quartz fiber membrane. The $^{63}Cu^{+}$ signal was largest on the PAA surface. Figures 4.7 and 4.8 depict the $^{63}Cu^{+}$ signal from the ablation of PAA immobilized quartz fiber at the anode and cathode, respectively.

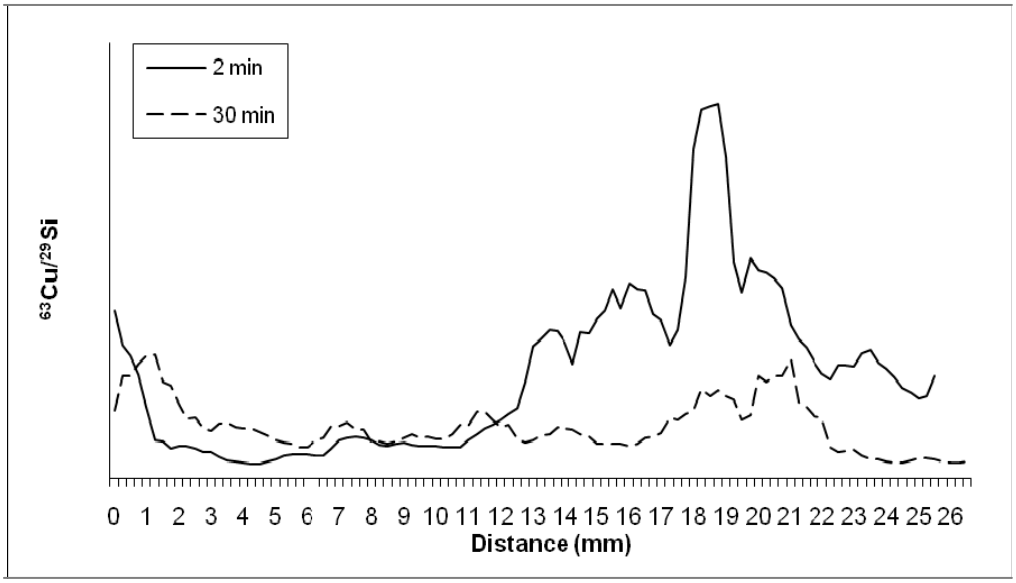

Figure 4.7. Cu signal monitored during 4 V electroblot on process on the anode side of the elctroblot. Ablation from a quartz fiber membrane chemically modified with PAA.

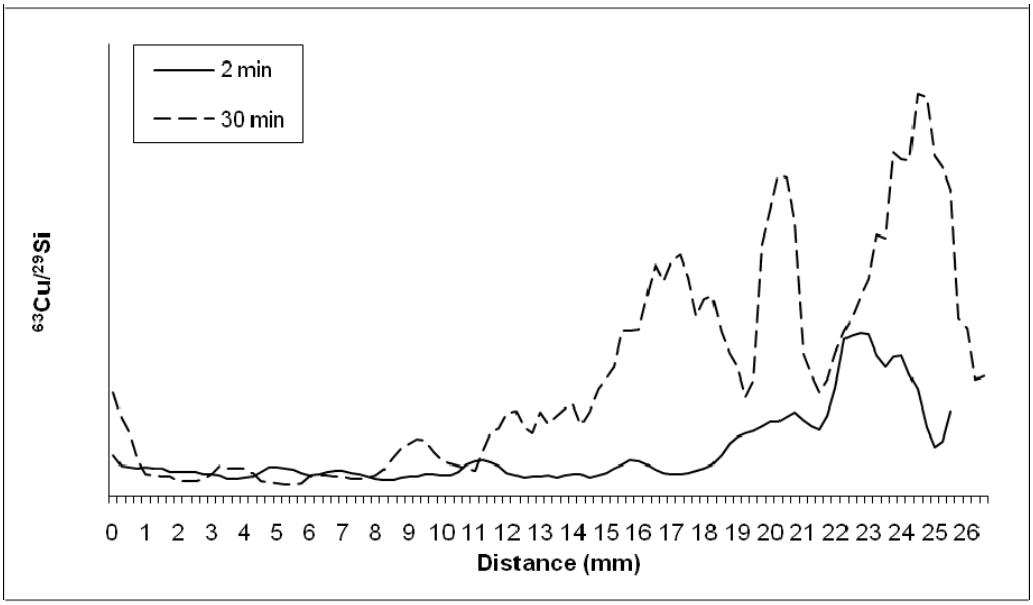

Figure 4.8. Cu signal monitored during 4 V electroblot on process on the cathode side of the elctroblot. Ablation from a quartz fiber membrane chemically modified with PAA.

At the anode membrane, $^{63}Cu^{+}$ decreases with time while increasing at the cathode. These results indicate improved Cu^{2+} capture by the carboxylate groups of the PAA on the metal capture side (cathode). However, the decrease in ^{63}Cu signal at the anode is unexpected, due to the larger Cu^{2+} affinity of PAA. One possibility is that the protein itself is filling the carboxylate sites of the PAA and thus reducing Cu^{2+} binding at the anode.

4.4 CONCLUSIONS

In many cases, the dissociation equilibrium between proteins and metals cannot be neglected when a separation technique is used to isolate the metalloprotein. This is in contrast to the relative ease of obtaining the correct association in cases of covalent attachments such as Se in selenoproteins or P in phosphorylated proteins. For potentially labile complexes such as the Cu-BSA used in these studies, adding Cu^{2+} to the PAGE separation's running buffer minimized dissociation during the lengthy separation. However, the excess copper in the gel significantly decreased the S/N when LA-ICPMS of the gel was used in the analysis. By performing an electroblot from a BN-PAGE, the excess free metal cations (e.g., Cu^{2+}) were separated from the Comassie-bound, negatively charged metalloprotein. From the results presented, BN-PAGE followed by a modified protein electroblot provided distinct advantages: 1) It facilitated the removal of background free metal ions and ions weakly adsorbed on the protein; and 2) it preconcentrated the protein onto the surface of the blot membrane, improving sensitivity. Chemical modification of the silica fiber, electroblot membrane surface displayed a significant improvement in protein capture efficiency over a more traditional electroblot surface. Specifically, the silanization modification which incorporated a thiol functionality showed significantly enhanced capture efficiency, especially for the protein.

Chemical modification with PAA offered improved Cu^{2+} capture efficiency and furnished additional insight into BSA-Cu equilibrium.

4.5 ACKNOWLEDGEMENTS

The authors would like to acknowledge the Norman Hackerman Advanced Research Program for funding support.

4.6 REFERENCES

1. J. Szpunar, *Anal. Bioanal. Chem.*, 2004, **378**, 54-56.

2. R. Lobinski, C. Moulin and R. Ortega, *Biochimie*, 2006, **88**, 1591-1604.

3. R. Lobinski, D. Schaumloffel and J. Szpunar, *Mass Spectrom. Rev.*, 2006, **25**, 255-289.

4. S. Mounicou, J. Szpunar and R. Lobinski, *Chem. Soc. Rev.*, 2009, **38**, 1119-1138.

5. H. Chassaigne, C. C. Chery, G. Bordin, F. Vanhaecke and A. R. Rodriguez, *Journal of Analytical Atomic Spectrometry*, 2004, **19**, 85-95.

6. J. L. Neilsen, A. Abildtrup, J. Christensen, P. Watson, A. Cox and C. W. McLeod, *Spectrochimica Acta, Part B: Atomic Spectroscopy*, 1998, **53B**, 339-345.

7. S. Lustig, D. Lampaert, K. De Cremer, J. De Kimpe, R. Cornelis and P. Schramel, *Journal of Analytical Atomic Spectrometry*, 1999, **14**, 1357-1362.

8. C. C. Chery, H. Chassaigne, L. Verbeeck, R. Cornelis, F. Vanhaecke and L. Moens, *Journal of Analytical Atomic Spectrometry*, 2002, **17**, 576-580.

9. J. S. Becker, S. F. Boulyga, J. S. Becker, C. Pickhardt, E. Damoc and M. Przybylski, *Int. J. Mass Spectrom.*, 2003, **228**, 985-997.

10. C. C. Chery, D. Guenther, R. Cornelis, F. Vanhaecke and L. Moens, *Electrophoresis*, 2003, **24**, 3305-3313.

11. M. Wind, I. Feldmann, N. Jakubowski and W. D. Lehmann, *Electrophoresis*, 2003, **24**, 1276-1280.

12. J. S. Becker, M. Zoriy, U. Krause-Buchholz, J. S. Becker, C. Pickhardt, M. Przybylski, W. Pompe and G. Roedel, *Journal of Analytical Atomic Spectrometry*, 2004, **19**, 1236-1243.

13. J. S. Becker, M. Zoriy, J. S. Becker, C. Pickhardt, E. Damoc, G. Juhacz, M. Palkovits and M. Przybylski, *Anal Chem*, 2005, **77**, 5851-5860.

14. J. S. Becker, M. Zoriy, C. Pickhardt, M. Przybylski and J. S. Becker, *Int. J. Mass Spectrom.*, 2005, **242**, 135-144.

15. C. C. Chery, L. Moens, R. Cornelis and F. Vanhaecke, *Pure Appl. Chem.*, 2006, **78**, 91-103.

16. U. Krause-Buchholz, J. S. Becker, M. Zoriy, C. Pickhardt, M. Przybylski, G. Roedel and J. S. Becker, *Int. J. Mass Spectrom.*, 2006, **248**, 56-60.

17. G. Ballihaut, S. Mounicou and R. Lobinski, *Anal. Bioanal. Chem.*, 2007, **388**, 585-591.

18. J. S. Becker, M. Zoriy, M. Przybylski and J. S. Becker, *Int. J. Mass Spectrom.*, 2007, **261**, 68-73.

19. M. Garijo Anorbe, J. Messerschmidt, I. Feldmann and N. Jakubowski, *Journal of Analytical Atomic Spectrometry*, 2007, **22**, 917-924.

20. A. Polatajko, M. Azzolini, I. Feldmann, T. Stuezel and N. Jakubowski, *Journal of Analytical Atomic Spectrometry*, 2007, **22**, 878-887.

21. M. S. Jimenez, L. Rodriguez, M. T. Gomez and J. R. Castillo, *Talanta*, 2010, **81**, 241-247.

22. J. S. Becker, S. Mounicou, M. V. Zoriy, J. S. Becker and R. Lobinski, *Talanta*, 2008, **76**, 1183-1188.

23. J. S. Becker, D. Pozebon, V. L. Dressler, R. Lobinski and J. S. Becker, *Journal of Analytical Atomic Spectrometry*, 2008, **23**, 1076-1082.

24. A. Raab, B. Pioselli, C. Munro, J. Thomas-Oates and J. Feldmann, *Electrophoresis*, 2009, **30**, 303-314.

25. I. Wittig and H. Schaegger, *Proteomics*, 2008, **8**, 3974-3990.

26. M. Howard, H. A. Jurbergs and J. A. Holcombe, *Journal of Analytical Atomic Spectrometry*, 1999, **14**, 1209-1214.

27. T. C. Miller and J. A. Holcombe, *J. Hazard. Mater.*, 2001, **83**, 219-236.

28. L. Malachowski and J. A. Holcombe, *Anal. Chim. Acta*, 2003, **495**, 151-163.

29. L. Malachowski and J. A. Holcombe, *Anal. Chim. Acta*, 2004, **517**, 187-193.

30. C. M. Halliwell and A. E. G. Cass, *Analytical Chemistry*, 2001, **73**, 2476-2483.

31. K. Hirayama, S. Akashi, M. Furuya and K. Fukuhara, *Biochem. Biophys. Res. Commun.*, 1990, **173**, 639-646.

32. W. Bal, J. Christodoulou, P. J. Sadler and A. Tucker, *J. Inorg. Biochem.*, 1998, **70**, 33-39.

33. J. Masuoka, J. Hegenauer, B. R. Van Dyke and P. Saltman, *J. Biol. Chem.*, 1993, **268**, 21533-21537.

34. P. K. C. Tseng and W. F. Gutknecht, *Analytical Chemistry*, 1975, **47**, 2316-2319.

35. J. Guo, N. Harn, A. Robbins, R. Dougherty and C. R. Middaugh, *Biochemistry*, 2006, **45**, 8686-8696.

36. R. J. P. Williams, *J. Inorg. Biochem.*, 2002, **88**, 241-250.

37. F. Despa, D. P. Orgill and R. C. Lee, *Ann. N. Y. Acad. Sci.*, 2005, **1066**, 54-66.

38. S. B. Zimmerman and S. O. Trach, *Journal of Molecular Biology*, 1991, **222**, 599-620.

Chapter 5: Summary and Future Directions

5.1 Using Internal Standardization for Improving Precision and Accuracy

Despite more than 30 years of research and routine analysis, it is important that work continue toward improving figures of merit for ICPMS. Because matrix matching is not always an option, care must be taken to avoid accuracy errors resulting from matrix-induced plasma aberrations. Based on the results presented in Chapters 2 and 3, internal standardization can offer improvements in both accuracy and precision. However, careful consideration must be taken to choose the best internal standard for a given analyte since a non-optimal pair may lead to exceedingly large errors in concentration, as illustrated in the evaluation series of Chapter 2.

A widely accepted practice among the ICPMS community is to choose analyte/internal standard pairs based on similarities in mass. However, the OLS calculations presented in Chapter 2 illustrate the large number of exceptions that exist. Unfortunately, the OLS models derived do not offer *a priori* selection based on similarities in the chemical properties considered. The low R^2 values indicate omitted chemical properties whose presence may lead to a more predictive model. Future studies should focus on including additional variables that may work toward *a priori* selection of internal standards.

Until a truly predictive model is realized, the database series detailed in Chapter 2 offers a unique approach to internal standard choice based on the minimization of analytical error. The program developed in Visual Basic offers a user-friendly interface that assists in internal standard choice based on matrix and/or operating conditions. Evaluation of the efficacy of this program is the major focus of Chapter 3. The results

presented in this chapter indicate that the database series is robust not only through instrument optimizations over time but, more importantly, over different instrument platforms.

5.2 EXPANDING ICPMS APPLICATIONS TO THE FIELD OF METALLOMICS

The vast majority of studies regarding protein-metal associations have focused on the characterization of a single metalloprotein. The ability to rapidly screen metalloproteins of a large mixture (ca. >100), although potentially powerful, has not been achieved. As discussed previously, the most effective separation technique for separating a large mixture of proteins is 2D PAGE with SDS as a charge shift molecule. A handful of early studies reported results utilizing SDS-PAGE,[1-5] neglecting to acknowledge potential metal loss and subsequent erroneous results. More recent studies using gel electrophoresis coupled with laser ablation ICPMS employ the less denaturing Coomassie Brilliant Blue™ as the charge shift molecule.[6-9] However, keeping the protein in its native form during the separation is only the tip of a proverbial iceberg. The idea of protein-metal equilibrium has been discussed in the literature. It has not, however, been addressed experimentally with respect to the free metal content of separation buffers prior to the study presented in Chapter 4. Some would argue that the free metal ion content of a cell is very low, negating the need for metal-loaded buffers. This argument neglects the well-studied concept of molecular crowding within a cellular environment. Approximately 60% of a cell's dry weight is comprised of proteins.[10] Two excellent review articles summarize work that has been done in this field.[11, 12] Molecular crowding can greatly affect the folding and unfolding mechanisms of proteins within a cell. It is reasonable to infer that this would alter the metal binding characteristics of metalloproteins, particularly with respect to kinetics. Molecular crowding also greatly impacts the activity of the components within a cell, with theoretical activity coefficients

of metal cations reaching 100.[13] Due to the complexity of this analytical challenge, emphasis in the literature has moved away from large protein mixtures and toward a more systematic approach utilizing a small number of well-characterized proteins.

Despite simplifying the system, it is clear from data presented in Chapter 4 that BSA does not retain the Cu^{2+} for extended periods of time in the presence of metal-free transfer buffer. Recent preliminary studies in our lab indicate that clear native PAGE results in improved ^{63}Cu S/N as well as a slightly reduced ^{107}Ag signal. The reduction of ^{107}Ag signal indicates a possible structural difference between Coomassie-bound and Coomassie-free BSA. The enhancement of ^{63}Cu signal may result from the fact that the strongest Cu-binding site of BSA contains histidine.[14] Since Coomassie binds to the basic and hydrophobic amino acid residues, there may be competitive binding between Coomassie and Cu^{2+}. More work is necessary to quantitate these differences in ^{63}Cu signal since they are reproducible but not large. Jimenz et al.[9] reported results for both clear native and blue native PAGE of alcohol dehydrogenase and superoxide dismutase. They did not report significant differences between the two, indicating that any issues with Coomassie are probably protein specific. To the best of the author's knowledge, no other study has directly compared the two native PAGE techniques with respect to metalloprotein metal loss. A rigorous comparison between the resolution of the two native PAGE techniques was published by Wittig et al.[15], concluding that BN-PAGE was significantly better.

Because of the decreased resolution of native-PAGE vs. SDS-PAGE, it is important for researchers to determine whether or not column separation is the better approach for metallomics applications. A column separation in lieu of PAGE would allow laser ablation to be replaced with pneumatic nebulization, immensely improving quantitative capabilities. Equilibrium considerations during the separation would be the

same, however, and metal loading the buffers would deteriorate S/N. The modified electroblot system detailed in Chapter 4 removes these background ions and may ultimately offer insight into protein-metal equilibrium and kinetics. Therefore, perhaps a more ideal system would be that which seamlessly integrates analysis from an electroblot surface with pneumatic nebulization. Work on this system has offered promising preliminary results in our laboratory.

5.3 REFERENCES

1. J. S. Becker, M. Zoriy, J. S. Becker, C. Pickhardt and M. Przybylski, *Journal of Analytical Atomic Spectrometry*, 2004, **19**, 149-152.

2. J. S. Becker, M. Zoriy, U. Krause-Buchholz, J. S. Becker, C. Pickhardt, M. Przybylski, W. Pompe and G. Roedel, *Journal of Analytical Atomic Spectrometry*, 2004, **19**, 1236-1243.

3. J. S. Becker, M. Zoriy, J. S. Becker, C. Pickhardt, E. Damoc, G. Juhacz, M. Palkovits and M. Przybylski, *Anal Chem*, 2005, **77**, 5851-5860.

4. J. S. Becker, M. Zoriy, C. Pickhardt, M. Przybylski and J. S. Becker, *Int. J. Mass Spectrom.*, 2005, **242**, 135-144.

5. J. S. Becker, M. Zoriy, M. Przybylski and J. S. Becker, *Int. J. Mass Spectrom.*, 2007, **261**, 68-73.

6. J. S. Becker, S. Mounicou, M. V. Zoriy, J. S. Becker and R. Lobinski, *Talanta*, 2008, **76**, 1183-1188.

7. J. S. Becker, D. Pozebon, V. L. Dressler, R. Lobinski and J. S. Becker, *Journal of Analytical Atomic Spectrometry*, 2008, **23**, 1076-1082.

8. A. Raab, B. Pioselli, C. Munro, J. Thomas-Oates and J. Feldmann, *Electrophoresis*, 2009, **30**, 303-314.

9. M. S. Jimenez, L. Rodriguez, M. T. Gomez and J. R. Castillo, *Talanta*, 2010, **81**, 241-247.

10. J. Li, S. Zhang and C.-C. Wang, *J. Biol. Chem.*, 2001, **276**, 34396-34401.

11. R. J. Ellis, *Trends in Biochemical Sciences*, 2001, **26**, 597-604.

12. F. Despa, D. P. Orgill and R. C. Lee, *Ann. N. Y. Acad. Sci.*, 2005, **1066**, 54-66.

13. S. B. Zimmerman and S. O. Trach, *Journal of Molecular Biology*, 1991, **222**, 599-620.

14. P. J. Sadler, A. Tucker and J. H. Viles, *Eur. J. Biochem.*, 1994, **220**, 193-200.

15. I. Wittig and H. Schaegger, *Proteomics*, 2008, **8**, 3974-3990.

References

Relevant references are listed at the end of each chapter.

Vita

Haley Joy Finley-Jones was raised in Albuquerque, NM where she graduated from Sandia High School in 2002. In 2006 she graduated from Northern Arizona University in Flagstaff, AZ with a B.S. in Chemistry. During her undergraduate career, she participated in metals analysis of tattoo inks under Dr. Jani C. Ingram. In addition to undergraduate research, Haley completed summer internships at the Harry Reid Center at the University of Nevada in Las Vegas and at Sandia National Laboratories in Albuquerque. In the fall of 2006, she attended The University of Texas at Austin to pursue a doctoral degree in analytical chemistry under the supervision of Professor James A. Holcombe.

Permanent address: 3452 Ridge Meadow St., Las Vegas, NV 89135

This dissertation was typed by the author.